

1 **Comprehensive analysis on the evolution characteristics and**
2 **causes of river runoff and sediment load in a mountainous basin**
3 **of China's subtropical plateau**

4 Xuchun Ye^{a*}, Chong-Yu Xu^b, Zengxin Zhang^c

5 ^a Chongqing Key Laboratory of Karst Environment & School of Geographical Sciences,
6 Southwest University, Chongqing 400715, China;

7 ^b Department of Geosciences, University of Oslo, P.O. Box 1047 Blindern, 0316 Oslo,
8 Norway;

9 ^c State Key Laboratory of Hydrology–Water Resources and Hydraulic Engineering, Hohai
10 University, Nanjing 210098, China;

11

12

13 *Corresponding author: Xuchun Ye

14 Address: 2 Tiansheng Road, Beibei District, Chongqing 400715, China.

15 e-mail: yxch2500@163.com

16 Tel: +86-15823497391

17 Email: yxch2500@163.com

18 ORCID: 0000-0001-8408-8318

19 **1 Introduction**

20 Runoff generation and sediment transport are the two complex dynamic processes in
21 surface water and soil systems, which are of essential importance for flood mitigation, river
22 channel training and river management (Chen *et al.*, 2001). Climate variability and human
23 activities in a river basin can result in alterations to the runoff and sediment processes.
24 Climate variability such as the increase of precipitation, may cause the increase of surface
25 runoff and the enhancement of soil erosion, and eventually leads to the increase of river
26 sediment. On the other hand, human activities such as land-use changes, urbanization, soil
27 conservation and dam construction, will lead to the change of river runoff and sediment in
28 time and space. During the past decades, 24% of the world's large rivers have experienced
29 significant changes in water flux and 40% in sediment flux, most notably declining trends
30 in water and sediment fluxes in Asia's large rivers and an increasing trend in suspended
31 sediment concentrations in the Amazon River (Li *et al.*, 2020). With the rapid development
32 of social economy, the impact of human activities on water and soil systems is increasingly
33 prominent. Since human disturbances cause substantial changes to the runoff and sediment
34 regimes, at present few rivers are in a natural state all over the world.

35 Rivers have a characteristic runoff regime that captures the typical pattern of
36 fluctuations in the magnitude, timing and frequency of runoff across a given year (Murphy,
37 2020). Under stationary climate and limited human influences, these fluctuations can be
38 expected within the ranges for a given runoff regime. However, runoff regime may be
39 changed systematically over time due to strong interference of natural and anthropogenic
40 factors. For example, mean runoff will increase when regional climate enters a humid
41 period, the frequency of large fluctuations of runoff events may decrease due to reservoir

42 construction or afforestation in the river basin (e.g. Ye et al., 2018). These changes in
43 runoff regime are of great significance for the understanding of long-term water-quality and
44 ecological alterations of river basins. In addition, the change of runoff regime may
45 eventually lead to the change of river sediment load due to the modification in processes of
46 sediment transport and riverbed erosion (Zhang et al., 2012; Wang et al., 2013; Yang et al.,
47 2015). In order to adopt water resources management and land planning, researches on the
48 evolution and driving mechanism of runoff and sediment under the changing environments
49 have been focused considerably on hydrology over the past decades (Zhang et al., 2006;
50 Gebremicael et al., 2013).

51 Quantitative assessment and separation of the impacts of climate variability and
52 human activities on runoff and sediment changes has always been an important hot issue.
53 Generally, there are two main approaches, process-based and statistical-based, were used to
54 evaluate the contributions of climate variability and human activities to streamflow change.
55 The former method mainly based on hydrological modelling by changing inputs of
56 meteorological and land use scenarios (Petchprayoon et al., 2010; Tesfa et al., 2014;
57 Madani et al., 2017; Li et al., 2019; Chen et al., 2019). Statistical method mainly includes
58 the empirical regression analysis and climate elasticity analysis. Especially, the climate
59 elasticity analysis, also known as hydrological sensitivity analysis, is a common method in
60 quantifying the influence of changes in precipitation and potential evaporation on
61 streamflow in recent years (Roderick and Farquhar, 2011; Ye et al., 2013; Wu et al., 2017).
62 Similarly, attempts to evaluate the impacts of climate variability and human activities on
63 river sediment change have been widely conducted (e.g. Tang et al., 2013; Zhao et al., 2017,
64 2018; Wei et al., 2017; Lacher et al., 2019; Murphy, 2020; Huang et al., 2020;
65 Martínez-Salvador & Conesa-García, 2019). Zhao et al. (2018) systematically reviewed six

66 quantitative methods in analyzing the response of sediment change to climate variability
67 and human activities, including the simple linear regression, double mass curve, sediment
68 identity factor analysis, dam-sedimentation based method, the Sediment Delivery
69 Distributed (SEDD) model, and the Soil Water Assessment Tool (SWAT) model. They
70 concluded that five methods produced similar estimates except for the linear regression
71 based on a case study in the Huangfuchuan watershed on the northern Loess Plateau. It is
72 worth noting that each method has its merits and disadvantages. Even though the most
73 popular process-based models (such as SWAT) have great applicability in evaluating the
74 impacts of climate variability and human activities on runoff and sediment processes, the
75 requirement of large amount of observed input data and low computational efficiency might
76 limit their wide application in those large river basins. Because that concentration (or load)
77 of annual mean sediment is related to annual streamflow conditions, in the attribution
78 analysis of sediment change, methodology of most researches is based on the statistical
79 relationship between sediment, runoff or precipitation (e.g. Wang et al., 2007; Li et al.,
80 2016; Zhao et al., 2018; Wu et al., 2019). For example, Murphy (2020) explored
81 contributions to sediment trends from changes in land management versus changes in the
82 streamflow regime through the analysis of concentration–streamflow relationship over time.
83 Actually, in this way, the impact factors of climate variability other than precipitation are
84 not well considered, or runoff itself is usually regarded as an impact factor, therefore the
85 relative role of climate variability and human activities cannot be clarified theoretically. Up
86 to now, scientists have been seeking for better approaches in quantifying the contributions
87 of climate variability and human activities on streamflow and sediment variations.

88 The Guizhou Province is a mountainous area in southwestern China. It is also one of
89 the main karst zones in the world (Parise et al., 2009). In this region, mountains and

90 plateaus are widely distributed and rivers are well developed. As a spatially open
91 double-layer hydrological system (Song et al., 2017), water and soil resources are easy to
92 be eroded from the surface and underground in karst area (Feng et al., 2016; Wang et al.,
93 2019b). For a long time, due to the influence of geological background and man-made
94 destruction, rocky desertification landscapes are widely distributed in the Guizhou province
95 (Cao et al., 2016; Yan et al., 2018). During the past decades, serious soil erosion in the
96 Guizhou province has led to barren soil, reduction of cultivated land area and frequent
97 droughts and floods, restricting the sustainable development of regional economy (Wang et
98 al., 2019a). Since the 1970s, extensive construction of hydropower stations has been
99 conducted in the river basins of the Guizhou Province (Wang et al., 2015). In recent years,
100 in order to control soil erosion and restore local ecology in the western China, a series of
101 China's national strategies have been implemented, such as the projects of ecological
102 environment construction and soil and water conservation in the middle and upper reaches
103 of the Yangtze River. These large scale human activities have considerably modulated river
104 discharge in time and space and reduced sediment load from hillslopes to river channels
105 (Xiong et al., 2008; Wang et al., 2015; Wu et al., 2018; Guan et al., 2019). Attributing
106 runoff and sediment trends to the effects of climate variability and human activities at the
107 catchment scale can provide a profound understanding of the relative contribution of
108 largely controllable human influences on river runoff and sediment, resulting from changes
109 in land management and surface disturbance, compared to that of less controllable changes
110 in the climate regime. The result of attribution analysis is critical for the sustainable
111 development of water resource and terrestrial ecosystems.

112 In this paper, we selected the Wujiang River basin (WRB), a large mountainous river
113 basin in Guizhou Province, southwestern China, as the study site for analyzing the

114 responses of annual runoff and sediment load to climate variability and human activities by
115 using an integrated approach. The objectives of this study are: (1) to present an integrated
116 approach for analyzing the evolution characteristics, including the trend, periodicity and
117 correlation of the runoff and sediment load over time; (2) to quantify the impacts of climate
118 variability and anthropogenic activities on the change of runoff and sediment load, and (3)
119 to link specific climate variability, implementation of soil and water conservation, and
120 extensive construction of hydropower stations to the changes of river runoff and sediment
121 load. This study provides a basic framework for analyzing the evolution characteristics and
122 causes of runoff and sediment load. What is particularly important is that we fully consider
123 the result of the attribution analysis of runoff change in quantifying sediment load changes.
124 Our results not only provide theoretical basis in guiding soil and water conservation and
125 local ecology restoration in the WRB, but also provide a good reference for the
126 comprehensive investigation of runoff and sediment changes in similar regions all over the
127 world.

128 **2 Materials and methods**

129 **2.1 Study area**

130 The Wujiang River, located in southwestern China, is one of the major tributaries in the
131 upstream basin of Yangtze River with an average annual flow of 1627 m³/s (Fig.1). The
132 river runs about 1037 km through the west, middle and northeast of Guizhou province and
133 discharges into the Three Gorges reservoir at Fuling District of Chongqing city. The
134 Wujiang River basin (WRB) covers an area of 87, 900 km², where 75.6% of the area is
135 covered by carbonate rocks (Xiong et al., 2008). Major landforms of the WRB are

136 mountain plateau, middle low mountains and hills. Average altitude of the basin is about
137 1160 m above mean sea level (a.m.s.l.) and it ranges from 160 to 2800 m a.m.s.l. There are
138 15 large tributaries in the basin, with the largest being Liuchong River, Maotiao River,
139 Qingshui River and Hongdu River. The upper, middle and lower reaches of the WRB are
140 bounded at Yachihe and Sinan hydro-stations (Fig. 1). Historically, the WRB is a moderate
141 soil erosion area in the upper reaches of the Yangtze River, with an average annual soil
142 erosion of 1187 t/km² (Guan et al., 2019). Due to spatial difference of soil erosion, river
143 sediment load mainly comes from the upper reaches of the WRB disproportionately.
144 According to observations, mean annual discharge at Yachihe is 350 m³/s, which is about
145 39% of the Sinan station and 22% of the Wulong station. However, mean annual sediment
146 yield in the upstream basin above Yachihe station is 1687×10⁴ t, which is about 77% of the
147 basin above Sinan station and 43% of the basin above Wulong station.

148
149
150

Fig. 1. Insert here

151 Climatically, the WRB belongs to a subtropical climate zone except some west
152 headwater areas with altitude above 2000 m a.m.s.l. Average annual precipitation of the
153 basin is 900–1400 mm and average annual temperature is 13.02–17.53°C. Annual
154 precipitation in the catchment shows a distinct wet and a dry season. More than 65% annual
155 precipitation is concentrated in the wet season from April to August (Fig. 1).

156 Due to large changes of surface elevation and strong cutting of the rivers, the WRB is
157 rich in hydropower resources. It is an important base for the "West-East Electricity
158 Transmission Project" in China. Potential hydropower of the whole basin is 10.43 million
159 KW, of which, the main stream of the Wujiang River is 5.80 million KW. Since the 1970s,
160 there are 11 cascade hydropower stations have been built on the main stream of the

161 Wujiang River (Fig. 1). Among which, the reservoir dam of Wujiangdu hydropower station
162 is 162 meters high, which is the largest high dam that has been built in the karst area of
163 China.

164 **2.2 Available data**

165 In this paper, we use data from Wulong hydro-station to investigate the characteristics of
166 hydrological and sediment changes in the whole WRB. The Wulong hydro-station, located
167 on the lower mainstream of the Wujiang River, is the outlet control hydro-station of the
168 whole basin with a gauging area of 83, 053 km². Annual series of runoff and suspended
169 sediment load of the Wulong station during 1970–2016 were collected from Changjiang
170 Sediment Bulletin 2016. The Changjiang Sediment Bulletin is published every year and can
171 be accessed freely on the website (<http://www.cjh.com.cn/en>). The monitoring of river
172 runoff was based on the standard current meter measurement (GB 50179-2015, 2015),
173 while the monitoring of suspended sediment load was based on the cross-section sampling
174 and the corresponding runoff data (GB/T 50159-2015, 2015). There are documents of
175 standard procedures used to collect runoff and sediment load data. All these were
176 completed by the local hydrological station. According to the observed water and sediment
177 processes, the daily, monthly and annual runoff and sediment load of the river can be
178 calculated.

179 Meteorological data from 12 weather stations across the WRB (see Fig. 1) were
180 obtained from National Climate Centre of China Meteorological Administration (CMA).
181 The data include daily precipitation, temperature (maximum, minimum and mean), relative
182 humidity, sunshine duration, and wind speed among others during the period 1970–2016,
183 and with no missing data on the variables. All the climate variables provided by CMA had

184 gone through a standard quality control process before delivery (QX/T 66-2007, 2007).
185 Based on the meteorological datasets, daily potential evaporation of the weather stations
186 was estimated by the Penman-Monteith equation (Allen et al., 1998) which is
187 recommended by the Food and Agriculture Organization (FAO) of the United Nations.
188 Daily precipitation and potential evaporation were aggregated to obtain annual data of each
189 weather station. In consideration of the large degree of variation in topography and the
190 uneven distribution of weather stations across the catchment, an area based weighting
191 method was used to calculate the average precipitation, potential evaporation for the whole
192 catchment. The weight coefficient, expressed by the percentage of the area represented by
193 each meteorological station, was calculated using the Thiessen Polygon method.

194 In addition, eight consecutive survey data of national forest resources of China
195 completed in 1973–1976, 1977–1981, 1984–1988, 1989–1993, 1994–1998, 1999–2003,
196 2004–2008, 2009–2013, respectively, were obtained from China Forestry Database. The
197 data collection of forest resources was mainly based on the method of fixed sample plot
198 survey. In recent years, the interpretation of satellite remote sensing image was applied as a
199 supplementary method. According the eight consecutive survey data of national forest
200 resources, the forest coverage data of each time in the Guizhou Province were then
201 extracted. In addition, the basic information, such as operation year and reservoir volume of
202 the major hydropower stations on the mainstream of Wujiang River, was also collected.

203 All the data used in the paper can be freely accessed in the supplementary files.

204 **2.3 Methodologies**

205 Fig. 2 shows the framework of this study to investigate the evolution characteristics and
206 causes of the runoff and sediment load in the WRB. Firstly, the evolution characteristics of

207 the annual runoff and sediment load including the trend, periodicity, change point and their
208 correlations were systematically analyzed by using the related methods based on the
209 observed data during the period 1970–2016. Secondly, according to the evolution
210 characteristics, annual runoff and sediment load time series were divided into a baseline
211 period and several changing periods. On this basis, the contributions of climate variability
212 and human activities on runoff change were first distinguished by using a widely applied
213 Budyko-based hydrological sensitivity method, and then the result was further applied in
214 the attribution analysis of river sediment load change.

215

216 **Fig. 2.** Insert here

217

218 **2.3.1 Identification and characterization of runoff and sediment regimes**

219 In this study, an ordinary linear regression method in the form of $\hat{y} = at + b$ and the least
220 squares method were applied to analyze the time trend of the annual runoff and sediment
221 load. In this equation, α and b are the regression coefficients with α estimates the slope
222 (change rate) and b represents the interception, t is an independent time variable, \hat{y} is
223 the dependent series of annual runoff or sediment load. The slope (α) of the regression
224 indicates the direction and magnitude of the temporal change: positive slopes ($\alpha > 0$) and
225 negative slopes ($\alpha < 0$). The significance of the linear trend was further estimated by the
226 Mann-Kendall test (Mann, 1945; Kendall, 1975).

227 The continuous wavelet transform (CWT) was applied to study the periodicity of annual
228 runoff and sediment load series of the WRB. The CWT is a signal processing method that
229 has been widely used for analyzing localized variations of power within a geophysical time

230 series (e.g., Torrence and Compo, 1998; Zhang et al., 2009; Ye et al., 2016). Through CWT
231 analysis, hydro-meteorological series can be decomposed into time–frequency space to
232 determine both the dominant modes of variability and how those modes vary in time
233 (Torrence and Compo, 1998). Due to good balance between time and frequency
234 localization, Morlet wavelet was chosen as a basic wavelet when applied the CWT method
235 (Ye et al., 2016).

236 The cumulative anomaly method, a non-linear statistical method to judge the change
237 trend of discrete data points, was applied to detect potential change point of
238 hydro-meteorological series. The kernel of cumulative anomaly is to judge the discrete
239 amplitude of the discrete data to its mean value. If the cumulative anomaly increases, it
240 indicates that the discrete data is larger than its mean value, otherwise the decrease of
241 cumulative anomaly indicates that the discrete data is smaller than its mean value (Ran et
242 al., 2010). If the curve of cumulative anomaly is composed by the two parts of increase and
243 decrease, then the break point of the change trend can be determined. In order to verify the
244 result from visual evaluation of this method, the T-test was further used to analyze the
245 mean difference before and after the change point (Joan, 1987).

246 In addition, the double mass analysis was applied to detect the changes of relationship
247 between precipitation, runoff and sediment load. The method was initially used to examine
248 the consistency of hydrological or meteorological data. In recent years, it has been widely
249 applied in the assessment of the response of river discharge/sediment load to climate
250 variability and human activities (e.g., Ma et al., 2012; Gao et al., 2017). The double mass
251 analysis is composed of cumulative values of two parameters plotted against one another
252 over a certain time span. Slope breaks in the curve may indicate the change in relationship
253 between the studied variables, which can be driven by various factors, such as urbanization,

254 revegetation or deforestation, soil and water conservation measures and climate variability.
255 Most importantly, the slope breaks are able to help determine the change point year of a
256 geophysical time series (Searcy and Hardison, 1960). Furthermore, the ANCOVA method
257 (Wright, 2011) was used to test the significance of the slope difference between the two
258 lines before and after the change points.

259 **2.3.2 Attribution analysis on the change of annual runoff**

260 For a natural basin, the water balance can be described as:

$$261 \quad P = ET + R + \Delta S / \Delta t \quad (1)$$

262 where P is precipitation, ET is actual evapotranspiration, R is runoff, and the unit of all the
263 above variables is $mm/year$ and ΔS is the change in basin water storage with unit of mm .
264 Over a long period of time (i.e., 10 years or more), ΔS can be reasonably assumed as zero.

265 Following the mathematical expression of Budyko-Fu (Fu, 1981), a famous
266 Budyko-type hypothesis in describing water and energy balances, the long-term mean
267 annual actual evapotranspiration (ET) can be estimated as follows:

$$268 \quad ET/P = 1 + \phi - (1 + \phi^m)^{1/m} \quad (2)$$

269 where ϕ is termed “dryness index”, which equals to ET_p/P (ET_p is potential
270 evaporation); m is empirical parameter that determines the shape of the Budyko-Fu curve
271 and reflects the impact of other factors such as land surface characteristics and climate
272 seasonality on water and energy balances (Li et al., 2013). The details of the equation can
273 be found in Fu (1981). The parameter m in Equation (2) can be calibrated by comparing the
274 long-term annual ET calculated from the observed P and R in the Equation (1).

275 Based on the principle of hydrologic sensitivity proposed by Milly and Dunne et al.
276 (2002), the change in runoff caused by climate variability (precipitation and potential

277 evaporation) can be approximated as follows:

$$278 \quad \Delta R_{clim} = \frac{\partial R}{\partial P} \Delta P + \frac{\partial R}{\partial ET_p} \Delta ET_p \quad (3)$$

279 where ΔP and ΔET_p are the average changes in precipitation and potential evaporation in
 280 two different periods, respectively; $\frac{\partial R}{\partial P}$ and $\frac{\partial R}{\partial ET_p}$ represent the sensitivity coefficients of
 281 runoff to precipitation and potential evaporation, and can be further expressed based on the
 282 formula of Budyko-Fu:

$$283 \quad \frac{\partial R}{\partial P} = (1 + \phi^m)^{1/m} - \phi(1 + \phi^m)^{\left(\frac{1}{m}-1\right)} \quad (4)$$

$$284 \quad \frac{\partial R}{\partial ET_p} = \phi^{(m-1)}(1 + \phi^m)^{\left(\frac{1}{m}-1\right)} - 1 \quad (5)$$

285 With the calculated ΔR_{clim} , the impact of human-induced change in runoff (ΔR_{hum})
 286 can therefore be obtained as:

$$287 \quad \Delta R_{hum} = \Delta R - \Delta R_{clim} \quad (6)$$

288 The relative contributions of climate variability and human activities on runoff change
 289 can be further expressed as:

$$290 \quad \eta_{clim-R} = \frac{\Delta R_{clim}}{|\Delta R|} \times 100\% \quad (7)$$

$$291 \quad \eta_{hum-R} = \frac{\Delta R_{hum}}{|\Delta R|} \times 100\% \quad (8)$$

292 where η_{clim-R} and η_{hum-R} are the percentages of the impact of climate variability and
 293 human activities on streamflow, respectively.

294 **2.3.3 Attribution analysis on the change of river sediment load**

295 The transport of river sediment is accompanied by runoff. Usually, annual sediment load of
 296 a river increases with annual river discharge because more water discharge will have more
 297 power to transport more sediment. Numerous researches have shown that there exists a

298 good correlation between the two variables (e.g., Zheng et al., 2012; Guo et al., 2017).
299 However, disturbance of human activities, especially tremendous influences from water
300 reservoirs will cause change of this correlation (Guan et al., 2019).

301 For a period when human activities are relatively weak (the baseline period), the
302 correlation between annual runoff and sediment load of a river can be simplified as:

$$303 \quad S_b = f(R_b) \quad (9)$$

304 where S_b and R_b are annual sediment load and runoff series, respectively. Normally, the
305 relationship can be described as a power function (e.g. Ran et al., 2009; Wu et al., 2019).

306 If the external environmental conditions continue, annual river sediment load in other
307 periods can be re-constructed as:

$$308 \quad S_{sim-c} = f(R_c) \quad (10)$$

309 where S_{sim-c} is the re-constructed sediment load and R_c is the observed runoff.

310 With reference to the baseline period, actual change of river sediment load in other
311 periods (ΔS) is given as:

$$312 \quad \Delta S = Ave_{S_p} - Ave_{S_b} \quad (11)$$

313 where Ave_{S_p} and Ave_{S_b} are average annual sediment load series in the other periods and
314 the baseline period, respectively.

315 Average change of sediment load caused by runoff change (ΔS_R) can be calculated as:

$$316 \quad \Delta S_R = Ave_{S_{sim-c}} - Ave_{S_b} \quad (12)$$

317 where $Ave_{S_{sim-c}}$ is the predicted average annual sediment load in the other periods.

318 It is known that runoff change itself is affected by climate variability and human
319 activities, therefore, the impact of climate variability on river sediment load (ΔS_{clim}) can be
320 further considered as:

321
$$\Delta S_{clim} = \Delta S_R \times \eta_{clim-R} \quad (13)$$

322 The impact of human-induced change in sediment load (ΔS_{hum}) can be obtained as:

323
$$\Delta S_{hum} = \Delta S - \Delta S_{clim} \quad (14)$$

324 The relative contributions of climate variability and human activities on sediment load
325 change can be expressed as:

326
$$\eta_{clim-S} = \frac{\Delta S_{clim}}{|\Delta S|} \times 100\% \quad (15)$$

327
$$\eta_{hum-S} = \frac{\Delta R_{hum}}{|\Delta S|} \times 100\% \quad (16)$$

328 where η_{clim-S} and η_{hum-S} are the percentages of the impact of climate variability and
329 human activities on sediment load, respectively.

330 **3 Results**

331 **3.1 Change patterns of annual runoff and sediment load**

332 **3.1.1 Annual trends and variability**

333 Fig.3 shows the variation of annual runoff depth and sediment load of Wulong station
334 during 1970–2016. It is obvious from the figure that both variables are characterized by
335 inter-decadal fluctuation. Annual runoff was relatively large from the mid-1970s to the
336 mid-1980s, and from the mid-1990s to the mid-2000s, while relatively small from the
337 mid-1980s to the mid-1990s, and from the mid-2000s to the mid-2010s. The maximum and
338 minimum of annual runoff depth were 829.59 mm and 346.41 mm respectively, which
339 occurred in 1977 and 2006. The variation of sediment load at Wulong station is more
340 prominent. Annual sediment load and its fluctuation were relatively large from 1970 to
341 mid-1980s, and then reduced remarkably until the earlier 2000s. Since the mid-2000s,

342 annual sediment load of Wulong station has been further reduced to a very small level, and
343 so does the variation amplitude. The maximum annual sediment load in 1977 was 2 orders
344 of magnitude larger than the minimum in 2013.

345 In terms of long-term trend, annual runoff depth of Wulong station showed a slight
346 decreasing, but non-significant trend ($p > 0.1$) at a linear rate of -17.2 mm every 10 years.
347 Annual sediment load, however, showed a significantly decreasing trend ($p < 0.01$) at a
348 linear rate of 901×10^4 t every 10 years.

349

350 **Fig. 3.** Insert here

351

352 **3.1.2 Periodic characteristics**

353 The analysis of wavelet power spectra demonstrates the pronounced inter-annual and
354 decadal variability of the runoff and sediment load of Wulong station. Continuous wavelet
355 power spectrum in Fig. 4a indicates that energy centers of frequency space are mainly
356 concentrated in 15 to 25 year bands, 5 to 10 year bands and < 5 year bands. This
357 observation demonstrates that there exist three possible periodicities for the annual
358 variability of runoff during 1970–2016. According to the result of wavelet variance, it is
359 clear that the average primary periodicity of runoff of Wulong station is about 22 years, and
360 the two secondary periodicities are 7 and 4 years, respectively (Fig. 4b). Further analysis
361 from the distribution patterns of wavelet power spectrum in Fig. 4a indicates that the runoff
362 of WRB has experienced a periodic evolution process of high, low, high, low, and high
363 during 1970–2016 at the scale of 22 years primary periodicity. By the end of 2016, the
364 WRB was still in the period of high runoff. However, the result from Fig. 4a also

365 demonstrates that the length of primary periodicity of 15–25 years shows a decreasing trend
366 during the study period. The medium length periodicity of 5–10 years disappeared during
367 1986-2008.

368

369 **Fig. 4.** Insert here

370

371 The result of continuous wavelet transform of sediment load is somewhat different
372 from that of runoff. As shown in Fig. 5a, the energy centers of frequency space are mainly
373 concentrated in 20 to 30 year bands and 5 to 10 year bands. Compared to the result of
374 runoff, only two periodic components can be identified for annual sediment load. Although
375 both have medium length periodicity of 5–10 years, the length of primary periodicity of
376 sediment load is little longer. In addition, the energy centers of both timescales weakened
377 gradually during the study period. Especially, energy centers in the timescale of < 5 year
378 has almost disappeared since 2010. Result from wavelet variance indicates that annual
379 sediment load of Wulong station exists a primary periodicity of 25 years, and a secondary
380 periodicity of 7 years (Fig. 5b).

381

382 **Fig. 5.** Insert here

383

384 **3.1.3 Step change characteristics**

385 In order to eliminate the unit limitation of data and facilitate the comparison of variables of
386 different units or magnitudes, we first use the Min-max normalization method (Ji et al.,
387 2016) to standardize the original data series. Fig.6 shows the cumulative anomaly curves of
388 the standardized sequence of precipitation in the WRB, and runoff depth and sediment load

389 at Wulong station during 1970–2016. It can be seen that the variation of cumulative
390 anomalies of annual precipitation and runoff is highly consistent. There are three change
391 points in 1984, 1994 and 2004 can be clearly detected from visual inspection. The trend of
392 annual precipitation and runoff sequences before and after the change points is obviously
393 opposite in sign. T-test further demonstrates that there are significant differences ($p < 0.05$)
394 in the mean values of runoff and sediment before and after the three change points. Take
395 the three step change years as the boundary, annual precipitation and runoff series in the
396 WRB can be divided into four stages of high, low, high and low during 1970–2016. This
397 result is very similar to that of the periodicity analysis of runoff in Fig. 4. In which, runoff
398 of the WRB has experienced two cycles of high and low during the study period. According
399 to the discrete amplitude (Fig. 6), the analysis of cumulative anomaly further indicates the
400 relative fluctuation of annual runoff was smaller than that of precipitation before 1984,
401 while it changed to be bigger afterwards. However, the differences of relative fluctuation
402 between annual precipitation and runoff during the two periods before and after 1984 were
403 not significant by the T-test.

404 Step change of annual sediment load of the WRB was also occurred in 1984 and 1994.
405 Different from annual precipitation and runoff, no change point can be observed at 2004.
406 Instead, a change point in 2000 was found. Similarly, the three change points were further
407 validated by the T-test ($p < 0.05$). The relative fluctuation of annual sediment load of the
408 WRB was much bigger than that of precipitation and runoff.

409

410

411

Fig. 6. Insert here

412 **3.1.4 Changes of relationship between precipitation, runoff and sediment load**

413 The calculated double mass curves of cumulative precipitation versus cumulative runoff,
414 and cumulative runoff versus cumulative sediment load are presented in Fig. 7. It is clear
415 from the figure that the slope of the curves changed in some places. Good linear
416 relationship between the two cumulative variables can be observed in the two sides of slope
417 breaks. From visual inspection, the results in Fig.7a show that there exists a slight slope
418 change in the cumulative curve of precipitation versus runoff, where the slope of the curve
419 decreased after 2005. However, the ANCOVA test demonstrates that the slope difference
420 between the two fitted lines before and after 2005 was significant ($p < 0.05$). The change of
421 the correlation between runoff and sediment load is quite prominent. Three major slope
422 change places can be observed in the cumulative curve of runoff versus sediment load
423 (Fig.7b). The potential change-points were occurred around 1983, 1995 and 2005. In the
424 initial period of 1970–1982, the slope of the curve was quite steep. While, it decreased
425 gradually in the following periods of 1983–1994, 1995–2004 and 2005–2016. Especially,
426 the slope of the curve during 2005–2016 was very small, and close to a horizontal line. The
427 ANCOVA test demonstrates that the slope difference between the fitted lines before and
428 after the change points were significant ($p < 0.05$).

429

430 **Fig. 7.** Insert here

431

432 The changed precipitation-runoff and runoff-sediment load relationships indicate
433 significant regime changes of runoff and sediment processes in the WRB during the study
434 period. Generally, this change is more prominent for sediment load. According to the
435 double mass curves, the slope of fitted linear lines in each segment represents the runoff

436 coefficient or sediment concentration during the corresponding time period. Result from
437 Fig. 6a indicates that runoff coefficient during 1970–2004 was about 0.536, while it
438 decreased to 0.491 after 2005. Sediment concentration was about 741 mg/L, 379 mg/L, 339
439 mg/L and 78 mg/L during the periods 1970–1982, 1983–1994, 1995–2004 and 2005–2016,
440 respectively. Mean concentration during the 1970–1982 period decreased by 362 mg/L on
441 the basis of the 1983–1994 period, and the number is 261 mg/L between the 1995–2004
442 period and the 2005–2016 period. The sediment decrease was more prominent for the
443 1983–1994 period, than for the 2005–2016 period.

444 **3.2 Runoff and sediment load changes in different periods**

445 In consideration of the results of both cumulative anomaly analysis and double mass
446 analysis, as well as the potential periodic characteristics, annual series of precipitation,
447 runoff and sediment load of the WRB during the study period can be divided into four
448 different periods: 1970–1984, 1985–1994, 1995–2004 and 2005–2016. Among them, the
449 basin was in a relatively wet period during 1970–1984 and 1995–2004, while the other two
450 periods were relatively dry. During the period 1970–1984, the relative fluctuation of runoff
451 was marginally less than that of precipitation (Fig. 6), which well reflects the natural
452 processes of rainfall-runoff in this karst basin. Variations of runoff and sediment load in the
453 other periods were obviously disturbed by more human activities.

454 Based on the above division of the four periods, the average value of runoff and
455 sediment in different periods was calculated. Result from Table 1 shows that annual runoff
456 and runoff coefficient were relatively larger in the period of 1970–1984 and the period of
457 1995–2004. During the period 2005–2016, both the runoff depth and runoff coefficient
458 were the minimum in the last four time periods. Average annual sediment load at Wulong

459 station was 3734×10^4 t during period of 1970–1984, while the value reduced dramatically
460 to 1604×10^4 t in the following period of 1985–1994. However, average annual sediment
461 load shows a slight increase in 1995–2004 with reference to the former period. In the period
462 2005–2016, average annual sediment load reduced to a very small value of 363.33×10^4 t.
463 Sediment concentration decreased gradually from 716 mg/L to 84 mg/L in the last four time
464 periods. Even in the period of 1995–2004 when sediment load increases relative to the
465 former period of 1985–1994, the sediment concentration still decreased.

466

467 **Table 1** Insert here

468

469 **3.3 Contribution of climate variability and human activities between periods**

470 **3.3.1 Runoff**

471 In the application of hydrologic sensitivity analysis method to runoff change attribution
472 analysis, m is a main model parameter. We calibrated m by comparing long-term annual ET
473 calculated by using Equation (2) and the water balance equation (1) for the relative natural
474 period 1970–1984. After manual trial and error, the optimized value of m is 1.71 for the
475 WRB. When $m=1.71$, the values of sensitivity coefficients $\partial R/\partial P$ and $\partial R/\partial ET_P$ were 0.72
476 and -0.29, respectively. This result reveals that the change in runoff was more sensitive due
477 to precipitation (P) than to potential evaporation (ET_P) in this region.

478 According to hydrological sensitivity analysis, all the calculated parameters were then
479 used to estimate the impact of climate variability on the change of runoff reference to the
480 baseline period 1970–1984. Table 2 lists the quantified result of the impacts of climate
481 variability and human activities separated by the method. As presented in Table 2, the

482 effects of climate variability and human activities varied in different periods. With
483 reference to the baseline period, the contribution rate of climate variability to the runoff
484 change was relatively large during the period 1985-1994. Both the contribution rates of
485 climate variability and human activities to runoff change were roughly the same between
486 the period 1995–2004 and the period 2005–2016, but their impact directions are different in
487 the two periods. Generally, quantified result indicates that with reference to the baseline
488 period 1970–1984, regional climate variability was always the main cause for runoff
489 change, not only in the relatively dry periods of 1985–1994 and 2005–2016, but also in the
490 relatively wet period of 1995–2004. In addition, climate variability and human activities
491 show the same effect direction on runoff change, both are positive or negative in the
492 changing periods.

493

494 **Table 2** Insert here

495

496 **3.3.1 Sediment load**

497 According to the annual variation of runoff and sediment load measured at Wulong station,
498 the functional correlation between the two variables was first established for the baseline
499 period 1970–1984. By comparing several kind of fitting functions (such as exponential
500 function; linear function; logarithmic function; polynomial function and power function),
501 the power function was finally confirmed to be the best fitting function in describing the
502 relationship between annual runoff and sediment load. As shown in Fig. 8, the fitted power
503 function for the baseline period was $S = 1.7283R^{1.2231}$ (where S and R are annual
504 sediment load and runoff with units of 10^4t and 10^8m^3). In the other periods, the fitted

505 power function was obviously changed. Overall, the fitted curve of power function in the
506 following three periods declined obviously, indicating that the sediment load measured at
507 Wulong station decreased significantly under the same runoff condition.

508

509 **Fig. 8.** Insert here

510

511 Table 3 lists the quantified impacts of climate variability and human activities on
512 sediment change in the WRB. With reference to the baseline period 1970–1984, it is
513 obvious from the table that human activities, rather than climate variability, dominate the
514 decrease of sediment load in the WRB. With reference to the baseline period, the average
515 reduction of annual sediment load was 2130×10^4 t in the period 1985–1994, the
516 contribution rate of climate variability was 32.8%, while that of human activities was
517 67.2%. In the following period 1995–2004, the average reduction of annual sediment load
518 was 1740×10^4 t. However, relative increment of sediment load due to runoff increase was
519 130.26×10^4 t, and so human activities resulted in a total reduction of 1870.26×10^4 t
520 sediment load. Therefore, the effect of climate variability to sediment load reduction is
521 negative, and the contribution rate was -7.5%, while the contribution of human activities
522 reached to 107.5%. In the period 2005–2016, the average reduction of annual sediment load
523 reached to extraordinary level 3370×10^4 t. The contribution rate of climate variability to the
524 sediment load reduction was 17.7%, and human activities was 82.3%.

525

526 **Table 3** Insert here

527

528 **4 Discussion**

529 Variations of annual runoff in the WRB are mainly influenced by natural factors, especially
530 precipitation changes. However, the source of river sediment mainly comes from slop soil
531 erosion of overland flow, the conditions of underlying surface such as vegetation cover,
532 topography, water conservancy project, etc. have important impacts on sediment load.
533 Normally, soil erosion on the slope more than 15° decreases obviously with the increase of
534 vegetation coverage (Wu et al., 2018). Generally, due to the special double-layer
535 hydrological system in the karst area, the underlying surface has limited effect on
536 regulating, storing and distributing precipitation, and soil and water resources are easy to be
537 lost in these processes (Song et al., 2017). Our observation revealed that the differences of
538 relative fluctuation between annual precipitation and runoff during the study period were
539 not significant (Fig. 6). This result further confirms that the underlying surface of the WRB
540 has a weak role in regulating and distributing precipitation. In the WRB, linear correlations
541 between annual precipitation and runoff were always significant during the study periods,
542 however, the linear correlations between annual precipitation and sediment load were not
543 significant during the periods of 1985–1994 and 2005–2016 (Fig. 9). The correlation
544 coefficient between precipitation and sediment load was considerably lower than that
545 between precipitation and runoff, indicating annual sediment loads incorporate additional
546 variability from sources other than precipitation, a large portion of which is attributable to
547 human activities.

548

549 **Fig. 9.** Insert here

550

551 Like many regions in China, the Guizhou Province has undergone intensive human

552 activities. Among which, the changes of land use/land cover and dam construction are the
553 two essential human activities that may have exerted considerable impacts on runoff and
554 sediment processes. The result of the eight continuous surveys of national forest resources
555 indicates that forest coverage of the Guizhou Province has changed greatly during the past
556 decades (Fig. 10). Because the Guizhou province is a typical karst mountainous region in
557 China, rock desertification is quite common and the overall forest coverage is low. Since
558 the 1960s, large-scale industrial and agricultural development has gradually started. Slope
559 planting in mountainous area and river valleys resulted in destruction of vegetation cover.
560 Forest coverage of the Guizhou Province dropped to the lowest level in the earlier 1980s
561 (Fig. 10). For this reason, sediment load of the Wujiang River was obviously higher during
562 the baseline period of 1970–1984. Since the mid-1980s, the implementation of soil and
563 water conservation has been carried out in the Guizhou Province, such as the projects of
564 slope farmland management, afforestation, returning farmland to forest and small water
565 conservancy construction (Zhang, 2016; Gu et al., 2018). In particular, the wide
566 implementation of slope farmland transformation and returning farmland to forest played
567 an important role in restraining soil erosion. During the past four decades, 84.51% area of
568 the WRB showed an increasing trend of vegetation coverage, especially in the
569 middle-lower basin, however, the area with decreasing trend of forest coverage mainly
570 distributed in the upper basin and along the riverside (Zheng et al., 2018). Relevant studies
571 revealed that human activities play a dominant role in the change of vegetation coverage in
572 WRB (Shi et al., 2017; Zheng et al., 2018). It should be noted that the initial work of water
573 and soil conservation and returning farmland to forest progressed slowly, and the effect on
574 reducing river sediment was not significant in the 1980s. For example, study by Wu et al.
575 (2018) pointed out that sediment load at Hongjiadu station was basically the same in 1970s

576 and 1980s under the same condition of river runoff. Only in the later 1990s, after a long
577 time period of soil and water conservation, can the condition of soil erosion in the basin be
578 greatly improved. Normally, it is a gradual process for human activities to affect river
579 discharge and sediment by changing the underlying surface of the river basin. After all,
580 large-scale basin development, soil and water conservation, and afforestation/deforestation
581 need many years to complete, and their impacts on runoff and sediment processes are
582 gradually increasing or decreasing.

583

584 **Fig. 10.** Insert here

585

586 It is known that most of the hydropower stations have limited influence on the
587 long-term change of river annual runoff, however, the construction of hydropower stations
588 on rivers can have an immediate impact on sediment load (Gao et al., 2011; Ibanez, 2015).
589 Up to now, there are 11 cascade hydropower stations have been completed and put into
590 operation on the mainstream of the Wujiang River (see in Fig. 1). Fig. 11 shows the
591 variation of cumulative reservoir volume according to the operation of the hydropower
592 stations. Because serious soil erosion and degradation of ecological environment in the
593 WRB are mainly concentrated in the upstream areas (Lu et al., 2018; Guan et al., 2019), the
594 operation of Wujiangdu hydropower station in 1982, Dongfeng hydropower station in 1994,
595 and Hongjiangdu hydropower station in 2004 was overall consistent with the sharp
596 reduction of sediment load and the changed relationship between runoff and sediment load
597 at Wulong station during the changing periods, indicating that the operation of hydropower
598 stations has a decisive impact on the interception of river sediment load.

599

Fig. 11. Insert here

600
601

602 The results of our investigation confirmed the earlier conclusion that human activities
603 (such as soil and water conservation, afforestation, hydropower station construction, etc.)
604 exert more influences on the change of annual sediment load than on runoff (Gao et al.,
605 2011; Ibanez, 2015). This result is quite common all over the world. Li et al. (2020)
606 revealed that the change of precipitation is found significantly correlated to the change of
607 water flux in 71% of the world's large rivers, while dam operation and irrigation rather
608 control the change of sediment flux in intensively managed catchments. It should be noted
609 that human activities have a positive effect of increasing runoff in the WRB during the
610 period 1995–2004 with reference to the baseline period, which is different from the result
611 of the other periods. The main reason lies in the serious destruction of the surface
612 vegetation due to the prevailing of hydropower station construction in the basin during this
613 period (Zheng et al., 2018; Guan et al., 2019). The slightly increased sediment load during
614 1995–2004 with reference to the former period of 1983–1994, also indicates the enhanced
615 soil erosion in this period.

616 Based on the above analysis, it is easy to understand the change patterns of annual
617 runoff and sediment load in the WRB. During 1970–2016, annual precipitation of the WRB
618 showed a slight decreasing trend. This well explains the decreasing trend of river runoff.
619 The increasing forest coverage, especially the construction of cascade hydropower stations
620 in the basin is obviously responsible for the significant reduction of sediment load. In the
621 Yangtze River basin, the periodicity of precipitation and runoff at different time scales has
622 been widely observed. For example, runoff in the Poyang Lake basin exhibits three
623 different timescales of periodicity: 25 year, 8 years and 3–4 years (Liu et al., 2009). Annual

624 precipitation in the upper Yangtze River basin mainly varies under the periodicity of 4, 7
625 and 15 years (Sun et al., 2012). The periodic characteristics of this inter-annual variation
626 are possibly correlated to the impacts of Asian monsoon and El Nino (Xiao et al., 2014;
627 Zhang, 2015; Wang et al., 2016). However, our investigation further demonstrates that the
628 length of the runoff periodicity of 15–25 years during the study period showed a decreasing
629 trend. This feature has not appeared in other researches, and the reasons behind deserve
630 further study. The periodicity of sediment load at Wulong station gradually weakened or
631 even disappeared, indicating strong influence of accumulation of sediment interception in
632 the reservoirs of hydropower stations.

633 In addition, the estimated step changes of precipitation and runoff according to
634 cumulative anomaly analysis were highly consistent with the 22 years primary periodicity
635 of runoff variation. This indicates that precipitation and runoff of the basin will change
636 significantly during different dry and wet periods. However, the occurrence of change point
637 for the correlations between precipitation, runoff and sediment load was somewhat different
638 from the results of cumulative anomaly analysis, especially for the correlation between
639 precipitation and runoff. The main reason is that the changes of precipitation and runoff are
640 highly synchronous. Therefore, when the two variables become smaller/larger in the same
641 proportion, the double mass curve is likely to keep the same slope so as to blur the possible
642 change point. The observed change point years from the double mass curve of runoff versus
643 sediment load are quite consistent with that of cumulative anomaly analysis. However, the
644 exact determination of change point year from the double mass curve is inevitably to be
645 arbitrary due to artificial inspection.

646 In this study, we provide a basic framework for analyzing the evolution characteristics
647 and causes of river runoff and sediment load which can be referred in other relevant

648 researches. Especially, we extend methods on previous studies by incorporating the result
649 of attribution analysis of the runoff change in the attribution analysis of river sediment load
650 change, which provides a new perspective for related research. In most of the previous
651 studies river runoff was regarded as one influence factor besides human activities on
652 sediment change attribution (e.g, Wang et al., 2007; Li et al., 2016; Guan et al., 2019;
653 Murphy, 2020). As we know, runoff change itself is affected by climate change and human
654 activities, and this impact will be more prominent under the context of intensified climate
655 variability and anthropogenic stresses (Li et al., 2020). With comparison to previous studies,
656 it is undoubtedly that the proposed method and quantified results in this paper have a better
657 theoretical significance in attributing causes to temporal changes in sediment. However,
658 there are also some weaknesses and uncertainties exist in our study. Firstly, we used
659 meteorological data from 12 weather stations in the WRB which might not be enough to
660 cover such a large basin with remarkable topographic changes. Secondly, the performance
661 of the hydrologic sensitivity analysis and the fitted function for annual runoff and sediment
662 load depends on the data of the baseline period, with no/limited effect of human activities.
663 In reality, during the baseline period of 1970-1984, there were still human disturbances in
664 WRB. Although the calibrated parameter (m) well reflects the average vegetation condition
665 of the catchment, and the fitted power function for annual runoff and sediment load passed
666 significant inspection during the baseline period, this could still affect the estimation results
667 to some extent. In addition, from a practical point of view, it would be much more
668 important to quantify the role of sediment accumulation in reservoirs and the role of
669 reducing erosion intensity in the river basin. However, due to the different operation time of
670 hydropower stations and the lack of long-term monitoring data of sediment load at the
671 outlet of each hydropower station, further separation is currently impossible in this paper

672 and leave for future studies.

673 **5 Conclusion**

674 In this study, we performed an integrated approach for analyzing the evolution
675 characteristics and causes of runoff and sediment load in a typical mountainous river basin,
676 the Wujiang River basin in southwestern China during 1970–2016. The main conclusions
677 are summarized as follows:

678 (1) The change patterns of runoff and sediment load were well revealed by the
679 integrated approach of trend, periodicity and step change. During the study period, annual
680 runoff at Wulong station shows a slight decreasing trend, while a significant decreasing
681 trend exists for sediment load. Annual runoff exists a primary periodicity of 22 years, and
682 the two secondary periodicities of 7 and 4 years. Annual sediment load exists a primary
683 periodicity of 25 years, and a secondary periodicity of 7 years. However, the length of the
684 primary periodicity of runoff showed a decreasing trend during the study period, both the
685 periodicities of sediment load weakened gradually or even disappeared in recent years. Step
686 changes of annual precipitation and runoff in the WRB were occurred in 1984, 1994 and
687 2004, while for annual sediment load were occurred in 1984, 1994 and 2000. The
688 relationships of precipitation-runoff and runoff-sediment load were also observed to be
689 changed in varying degrees.

690 (2) We extend methods on previous studies by incorporating the result of attribution
691 analysis of the runoff change in the attribution analysis of river sediment load change,
692 which provides a new perspective for related research. Quantitative assessment revealed
693 that climate variability contributes 71.5% ~ 85.6% changes of mean annual runoff in
694 1985–1994, 1995–2004 and 2005–2016, with reference to the baseline period of

695 1970–1984, while human activities play a secondary role. In contrary, human activities (e.g.
696 soil and water conservation, afforestation, construction of water reservoirs) dominate the
697 reduction of river sediment load in the three periods, and the contribution rate ranged in
698 67.2% ~ 107.5%.

699 (3) The construction of cascade hydropower stations in the WRB was fundamentally
700 responsible for the significant decreasing trend and the weakened periodicity of sediment
701 load as well as the changed runoff-sediment load relationship at Wulong station in recent
702 years. However, this influence was not big enough to modify the regime of annual runoff in
703 the WRB.

704 **Acknowledgements**

705 This work was financially supported by the Fundamental Research Funds for the Central
706 Universities (XDJK2019B074) and the National Natural Science Foundation of China
707 (42071028). Cordial thanks go to two anonymous reviewers for their valuable comments
708 and suggestions that greatly improved the quality of this paper.

709 **References**

- 710 Allen, R.G., Pereira, L.S., Raes, D., Smith, M., 1998. Crop Evapotranspiration Guidelines for
711 Computing Crop Water Requirements. FAO Irrigation and Drainage Paper No. 56. FAO, Rome.
- 712 Cao, J., Hu, B., Grovers, C., Huang, F., Yang, H., Zhang, C., 2016. Karst dynamic system and the carbon
713 cycle. *Z. Geomorphol.* 60 (Suppl. 2), 35–55.
- 714 Chen, L., Chang, J.X., Wang, Y.M., Zhu, Y.L., 2019. Assessing runoff sensitivities to precipitation and
715 temperature changes under global climate-change scenarios. *Hydrol. Res.* 50 (1), 24–42.
- 716 Chen, Z., Li, J., Shen, H., Wang, Z., 2001. Yangtze River of China: historical analysis of discharge
717 variability and sediment flux. *Geomorphology*, 41, 77–91.

718 Feng, T., Chen, H., Polyakov, V.O., Wang, K., Zhang, X., Zhang W., 2016. Soil erosion rates in two karst
719 peak-cluster depression basins of northwest Guangxi, China: comparison of the RUSLE model with
720 $^{137}\text{C}_s$ measurements. *Geomorphology*, 253, 217–224.

721 Fu, B.P., 1981. On the calculation of the evaporation from land surface. *Chinese Journal of Atmospheric*
722 *Sciences*, 5, 23–31. (in Chinese)

723 Gao, P., Li, P., Zhao, B., Xu, R., Zhao, G., Sun, W., Mu, X., 2017. Use of double mass curves in
724 hydrologic benefit evaluations. *Hydrol. Process.* 31(16), 4639–4646.

725 Gao, P., Mu, X., Wang, F., Li, R., 2011. Changes in streamflow and sediment discharge and the response
726 to human activities in the middle reaches of the Yellow River. *Hydrol. Earth Syst. Sci.* 15(1), 1–10.

727 GB 50179-2015, 2015. Code for liquid flow measurement in open channels (National standards of the
728 People’s Republic of China). China Planning Press, pp. 11–25. (in Chinese)

729 GB/T 50159-2015, 2015. Code for measurements of suspended sediment in open channels (National
730 standards of the People’s Republic of China). China Planning Press, pp. 21–42. (in Chinese)

731 Gebremicael, T.G., Mohamed, Y.A., Betrie, G.D., van der Zaag, P., Teferi, E., 2013. Trend analysis of
732 runoff and sediment fluxes in the Upper Blue Nile basin: A combined analysis of statistical tests,
733 physically-based models and landuse maps. *J. Hydrol.* 482(9), 57–68.

734 Gu, Z., Yang, Y., Wang, X., 2018. Achievements and experiences of soil and water conservation in
735 Guizhou Province in the past 40 years of reform and opening up. *Soil and water conservation of*
736 *China*, 441 (12), 67–70. (in Chinese)

737 Guan, X., Xiang, X., Li, C., Wang, Z., 2019. Analysis of evolution characteristics and driving factors of
738 annual runoff and sediment transportation changes in Wujiang River. *Journal of Sediment Research*,
739 44(5), 36–41. (in Chinese)

740 Guo, X., Li, T., He, B., He, X., Yao, Y., 2017. Effects of land disturbance on runoff and sediment yield
741 after natural rainfall events in southwestern China. *Environ. Sci. Pollut. R.* 24(10), 1–10.

742 Huang, L.D., Ye, A.Z., Tang, C.J., Duan, Q.Y., Zhang, Y.H., 2020. Impact of rural depopulation and
743 climate change on vegetation, runoff and sediment load in the Gan River basin, China. *Hydrol. Res.*
744 51(4), 768–780.

745 Ibanez, C., 2015. Changes in the hydrology and sediment transport produced by large dams on the lower
746 Ebro River and its estuary. *River Research & Applications*, 12, 51–62.

747 Ji, X., Du, S., Wang, G., 2016. Using min-max normalization to measure the differences of regional
748 economic growth—a case study of Yulin area, Shanxi Province. *Economy and Management*, 30(3),
749 54–56. (in Chinese)

750 Joan, F.B., 1987. Guinness, Gosset, Fisher, and Small Samples. *Statistical Science*. 2 (1), 45–52.

751 Kendall, M.G., 1975. *Rank Correlation Methods*. Griffin, London.

752 Lacher, I. L., Ahmadisharaf, E., Fergus, C., Akre, T., Mcshea, W. J., Benham, B. L., and Kline, K. S.,
753 2019. Scale-dependent impacts of urban and agricultural land use on nutrients, sediment, and runoff,
754 *Sci. Total Environ.*, 652, 611–622.

755 Li, D., Pan, M., Cong, Z., Zhang, L., Wood, E., 2013. Vegetation control on water and energy balance
756 within the Budyko framework. *Water Resour. Res.* 49(2), 969–976.

757 Li, L., Ni, J., Chang, F., Yue, Y., Frolova, N., Magritsky, D., Borthwick, A.G.L., Ciais, P., Wang, Y.,
758 Zheng, C., Walling, D.E., 2020. Global trends in water and sediment fluxes of the world's large
759 rivers. *Science Bulletin*, 65(1), 62–69.

760 Li, Y.Y., Chang, J.X., Luo, L.F., Wang, Y.M., Guo, A.J., Ma, F., Fan, J.J., 2019. Spatiotemporal impacts
761 of land use land cover changes on hydrology from the mechanism perspective using SWAT model
762 with time-varying parameters. *Hydrol. Res.* 50(1), 244–261.

763 Li, Z., Xu, X., Yu, B., Xu, C., Liu, M., Wang, K., 2016. Quantifying the impacts of climate and human
764 activities on water and sediment discharge in a karst region of southwest China. *J. Hydrol.* 542,
765 836–849.

766 Liu, J., Zhang, Q., Xu, C., Zhang, Z., 2009. Characteristics of Runoff Variation of Poyang Lake
767 Watershed in the Past 50 Years. *Tropical Geography*, 93(3):213–218. (in Chinese)

768 Lu, Y., Yang, X.D., Yang, Z.Y., 2018. Evaluation on Eco-environmental Quality Change of Wujiang
769 River Basin in Guizhou Province from 1990 to 2015. *Bulletin of Soil and Water Conservation*,
770 38(2), 140–147. (in Chinese)

771 Ma, X., Bai, H., Hou, Q., Yuan, B., Zhang, J., 2012. Runoff change of Bahe River basin in Qinling

772 mountains and its influencing factors. *Resources Science*, 34(7): 1298–1305. (in Chinese)

773 Madani, E.M., Jansson, P.E., Babelon, I., 2017. Differences in water balance between grassland and
774 forest watersheds using long-term data, derived using the CoupModel. *Hydrology Research* 49 (1),
775 72-89.

776 Mann, H.B., 1945. Nonparametric Tests against Trend. *Econometrica*, 13, 245–259.

777 Martínez-Salvador, A., Conesa-García, C., 2019. Estimation of suspended sediment and dissolved solid
778 load in a Mediterranean semiarid karst stream using log-linear models. *Hydrol. Res.* 50(1), 43-59.

779 Milly, P.C.D., Dunne, K.A., 2002. Macroscale water fluxes 2. Water and energy supply control of their
780 inter-annual variability. *Water Resour. Res.* 38, 241–249.

781 Murphy, J. C., 2020. Changing suspended sediment in United States rivers and streams: linking sediment
782 trends to changes in land use/cover, hydrology and climate. *Hydrology and Earth System Sciences*,
783 24(2), 991–1010.

784 Parise, M., de Waele, J., Gutierrez, F., 2009. Current perspectives on the environmental impacts and
785 hazards in karst. *Environ. Geol.* 58 (2), 235–237.

786 QX/T 66-2007. 2007. Specifications for surface meteorological observation. Part22: Quality control of
787 data (Meteorological industry standard of the People’s Republic of China). China Meteorological
788 Press, pp. 1–7. (in Chinese)

789 Ran, L.S., Wang, S.J., Fan, X.L., 2010. Channel change at Toudaoguai station and its responses to the
790 operation of upstream reservoirs in the upper Yellow River. *J. Geogr. Sci.* 20(2), 231–247.

791 Petchprayoon, P., Blanken, P.D., Ekkawatpanit, C., Hussein, K., 2010. Hydrological impacts of land
792 use/land cover change in a large river basin in central–northern Thailand, *Int. J. Climatol.* 30,
793 1917–1930.

794 Ran, D., Guo, B., Zhang, X., Wang, C., Dong, F., 2009. Analysis on variation and response of incoming
795 sediment coefficient of the Jinghe River basin. *J. Sediment Res.* 2009, 2, 60–67. (in Chinese)

796 Restrepo, J. C., Schrottke, K., Bartholomae, A., Ospino, S., Ortíz, J. C., Otero, L., Rondón, A.F.O., 2018.
797 Estuarine and sediment dynamics in a microtidal tropical estuary of high fluvial discharge:
798 Magdalena River (Colombia, South America). *Mar. Geol.* 398, 86–98.

799 Roderick, M.L., Farquhar, G.D., 2011. A simple framework for relating variations in runoff to variations
800 in climatic conditions and catchment properties, *Water Resour. Res.* 47(12), 667–671.

801 Searcy, J.K., Hardison, C.H., 1960. Double-mass Curves. U.S. Geological Survey Water Supply
802 Paper.1541–B.

803 Shi, Y.Y., Yin, Z.T., Zheng, W.F., 2017. Study on the response of vegetation cover change and climate
804 change in Wujiang River basin based on MODIS data. *Forest Resources Management*, 2017, 2(1),
805 127–134. (in Chinese)

806 Song, X., Gao, Y., Green, S.M., Dungait, J.A.J., Peng, T., Quine, T.A., Xiong, B., Wen, X., He N., 2017.
807 Nitrogen loss from karst area in China in recent 50 years: an in-situ simulated rainfall experiment's
808 assessment. *Ecol. Evol.*, 7 (23), 10131–10142.

809 Sun, J., Lei, X., Jiang, Y., Wang, Hao., 2012. Variation Trend Analysis of Meteorological Variables and
810 Runoff in Upper Reaches of Yangtze River. *Water Resources and Power*, 30(5), 1–4. (in Chinese)

811 Tang, Q., He, X.B., Bao, Y.H., Zhang, X.B., Guo, F., Zhu, H.W., 2013. Determining the relative
812 contributions of climate change and multiple human activities to variations of sediment regime in
813 the Minjiang River, China. *Hydrol. Process.* 27, 3547–3559.

814 Tesfa, T.K., Li, H. Y., Leung, L. R., Huang, M., Ke, Y., Sun, Y., Liu, Y., 2014. A Subbasin–based
815 framework to represent land surface processes in an Earth System Model. *Geosci. Model Dev.* 7,
816 947–963.

817 Torrence, C. & Compo, G. P. 1998. A practical guide to wavelet analysis. *Bull. Am. Meteor. Soc.* 79 (1),
818 61–78.

819 Wang, J., Sheng, Y., Gleason, C.J., Wada, Y., 2013. Downstream Yangtze River levels impacted by Three
820 Gorges Dam. *Environ. Res. Lett.*, 8(4): 044012. DOI: 10.1088/1748-9326/8/4/044012.

821 Wang, M.M., Wang, S.J., Bai, X.Y., Li, S.J., Li, H.W., Cao, Y., Xi, H.P., 2019a. Evolution characteristics
822 of karst rocky desertification in typical small watershed and the key characterization factor and
823 driving factor. *Acta Ecologica Sinica*, 39(16), 6083–6097. (in Chinese)

824 Wang, P., Shen, L.C., Chen, X.H., Wang, Z.J., Liang, X., Hu, B., Lan, J.C., Zhai, X.X., 2019b. Response
825 of soil water hydrochemistry and $\delta^{13}\text{C}_{\text{DIC}}$ to changes in spatio-temporal variations under different

826 land covers in SW China karst catchment. *Hydrol. Res.* 50(3), 925-944.

827 Wang, Y., Zhang, Q., Zhang, S., Chen, X., 2016. Spatial and Temporal Characteristics of Precipitation in
828 the Huaihe River Basin and Its Response to ENSO Events. *Scientia Geographica Sinica*, 36(1),
829 128–134. (in Chinese)

830 Wang, H., Yang, Z., Saito, Y., Liu, J.P., Sun, X., Wang, Y. 2007. Stepwise decreases of the Huanghe
831 (Yellow River) sediment load (1950–2005): Impacts of climate change and human activities. *Global*
832 *Planet. Change*, 57(3-4): 331–354.

833 Wei, Y.H., He, Z., Li, Y.J., Jiao, J.Y., Zhao, G.J., Mu, X.M., 2017. Sediment yield deduction from
834 check-dams deposition in the weathered sandstone watershed on the North Loess Plateau, China.
835 *Land Degrad. Dev.* 28, 217–231.

836 Wright, D.B., 2011. Comparing groups in a before – after design: When t test and ANCOVA produce
837 different results. *Brit. J. Educ. Psychol.* 76(Pt 3), 663–675.

838 Wu, C., Ji, C., Shi, B., Wang, Y., Gao, J., Yang, Y., Mu, J., 2019. The impact of climate change and
839 human activities on streamflow and sediment load in the Pearl River basin. *Int. J. Sediment Res.* 34:
840 307–321.

841 Wu, J., Miao, C., Wang, Y., Duan, Q., Zhang, X., 2017. Contribution analysis of the long-term changes
842 in seasonal runoff on the Loess Plateau, China, using eight Budyko-based methods. *J. Hydrol.* 545,
843 263–275.

844 Wu, X.L., Zhang, X., Xiang, X.H., Chen, X., Wang, C., Li, X., 2018. Runoff and sediment variations in
845 the upstream of Wujiang River Basin and the influences of hydropower station construction.
846 *Chinese Journal of Ecology*, 37(3):642–650. (in Chinese)

847 Xiao, W., Yong, P., Yong, N., Ji, F., 2015. Study on the cumulative effects of cascading reservoirs in
848 Wujiang. *Science Technology and Engineering*, 15(3), 275–279. (in Chinese)

849 Xiao, M., Zhang, Q., Singh, V.P., 2014. Influences of ENSO, NAO, IOD and PDO on seasonal
850 precipitation regimes in the Yangtze River basin, China. *Int. J. Climatol.* 35(12), 3556–3567.

851 Xiong, Y., Zhang, K., Yang, G., Gu, Z., 2008. Change in characteristics of runoff and sediment in the
852 Wujiang River. *Ecology and Environment*, 17(5), 1942–1947. (in Chinese)

853 Yang, S.L., Xu, K.H., Milliman, J.D., Yang, H.F., Wu, C.S., 2015. Decline of Yangtze River water and
854 sediment discharge: Impact from natural and anthropogenic changes. *Sci. Rep-UK*, 5, 12581.

855 Yan, Y., Dai, Q., Yuan, Y., Peng, X., Zhao, L., Yang, J., 2018. Effects of rainfall intensity on runoff and
856 sediment yields on bare slopes in a karst area, SW China. *Geoderma*, 330, 30–40.

857 Ye, X., Zhang, Q., Liu, J., Li, X., Xu, C., 2013. Distinguishing the relative impacts of climate change
858 and human activities on variation of streamflow in the Poyang Lake catchment, China. *J. Hydro.*
859 494(12), 83–95.

860 Ye, X., Li, X., Xu, C. Y., Zhang, Q., 2016. Similarity, difference and correlation of meteorological and
861 hydrological drought indices in a humid climate region – the Poyang Lake catchment in China.
862 *Hydrology research*. 47(6), 1211–1223.

863 Ye, X., Xu, C.Y., Li, X., Zhang, Q., 2018. Investigation of the complexity of streamflow fluctuations in a
864 large heterogeneous lake catchment in China. *Theor. Appl. Climatol.* 132, 751–762.

865 Zhang, L., Ding, M.J., Zhang, H.M., Wen, C., 2018. Spatiotemporal variation of the vegetation coverage
866 in Yangtze River Basin during 1982-2015. *Journal of Natural Resources*, 33(12), 2084–2097. (in
867 Chinese)

868 Zhang, X., 2016. History, achievements, problems and suggested countermeasures of karst
869 desertification control in Guizhou. *Carsologica Sinica*, 35(5), 497–502.

870 Zhang, Q., Li, L., Wang, Y., Werner, A.D., Xin, P., Jiang, T., Barry, D.A., 2012. Has the Three-Gorges
871 Dam made the Poyang Lake wetlands wetter and drier? *Geophys. Res. Lett.*, 39(20), L20402, 7pp.
872 DOI:10.1029/2012GL053431.

873 Zhang, Q., Xu, C.Y., Zhang, Z., Chen, Y. D., Liu, C. L., 2009. Spatial and temporal variability of
874 precipitation over China, 1951–2005. *Theor. Appl. Climatol.* 95 (1–2), 53–68.

875 Zhang, Q., Xu, C.Y., Becker, S., Jiang, T., 2006. Sediment and runoff changes in the Yangtze River basin
876 during past 50 years. *J. Hydrol.* 331(3-4): 511–523.

877 Zhao, G.J., Kondolf, G.M., Mu, X.M., Han, M.W., He, Z., Rubin, Z., 2017. Sediment yield reduction
878 associated with land use changes and check dams in a catchment of the Loess Plateau, China.
879 *Catena* 148, 126–137.

- 880 Zhao, G., Mu X., Jiao J., Gao, P., Sun, W., Li, E., Wei, Y., Huang, J., 2018. Assessing response of
881 sediment load variation to climate change and human activities with six different approaches.
882 Science of the Total Environment, 639, 773–784.
- 883 Zheng, H., Fang, S., Yang, J., Xie, S., Chen, X., 2012. Analysis on evolution characteristics and
884 impacting factors of annual runoff and sediment in the Ganjiang River during 1970-2009. Journal
885 of Soil & Water Conservation, 26(1), 28–32. (in Chinese)
- 886 Zhang, R., 2015. Changes in East Asian summer monsoon and summer rainfall over eastern China
887 during recent decades. Science Bulletin, 13, 88–90. (in Chinese)

Xuchun Ye: Conceptualization, Investigation, Writing - Original Draft.

Chong-Yu Xu: Validation, Writing- Reviewing and Editing.

Zengxin Zhang: Software, Resources.

Declaration of Interest Statement:

The authors declared that they have no conflicts of interest to this work.

Cover letter

Dear Editor,

We thank the referees for their additional comments in the second round of review, which have been a great help in improving the quality of our paper. We carefully revised the paper according to these comments and suggestions. The related parts of the paper have been rewritten and improved, and for your easy reading and evaluation, the changed parts are marked using RED COLORED text in the revised version.

We hope the revised version is to your satisfaction, and of course, we are more than happy to improve the paper again according to new comments and suggestions they might come.

Thank you in advance for your considerations.

Sincerely Yours

Xuchun Ye

on behalf of the co-authors,

Figure 1
[Click here to download high resolution image](#)

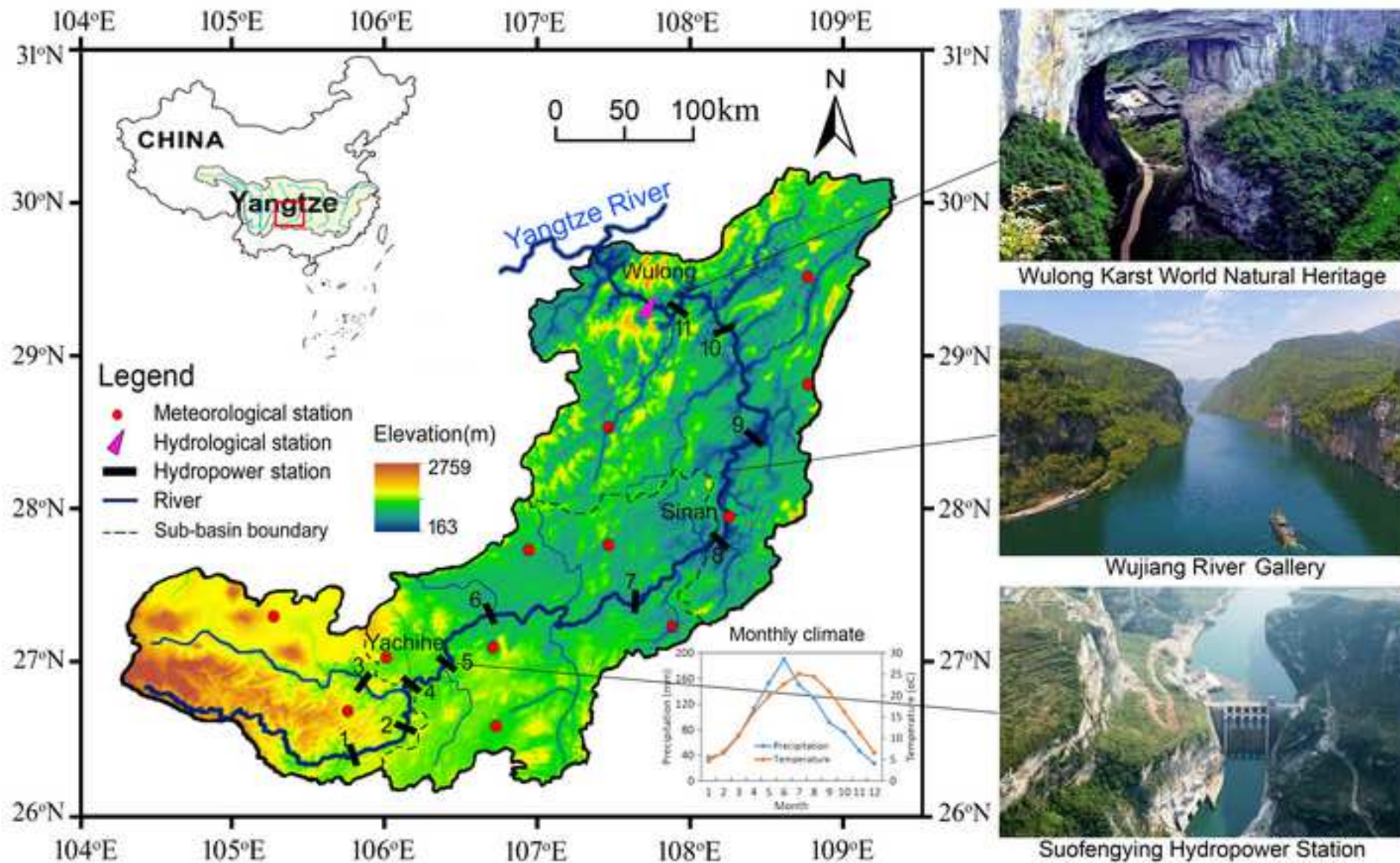


Figure 2
[Click here to download high resolution image](#)

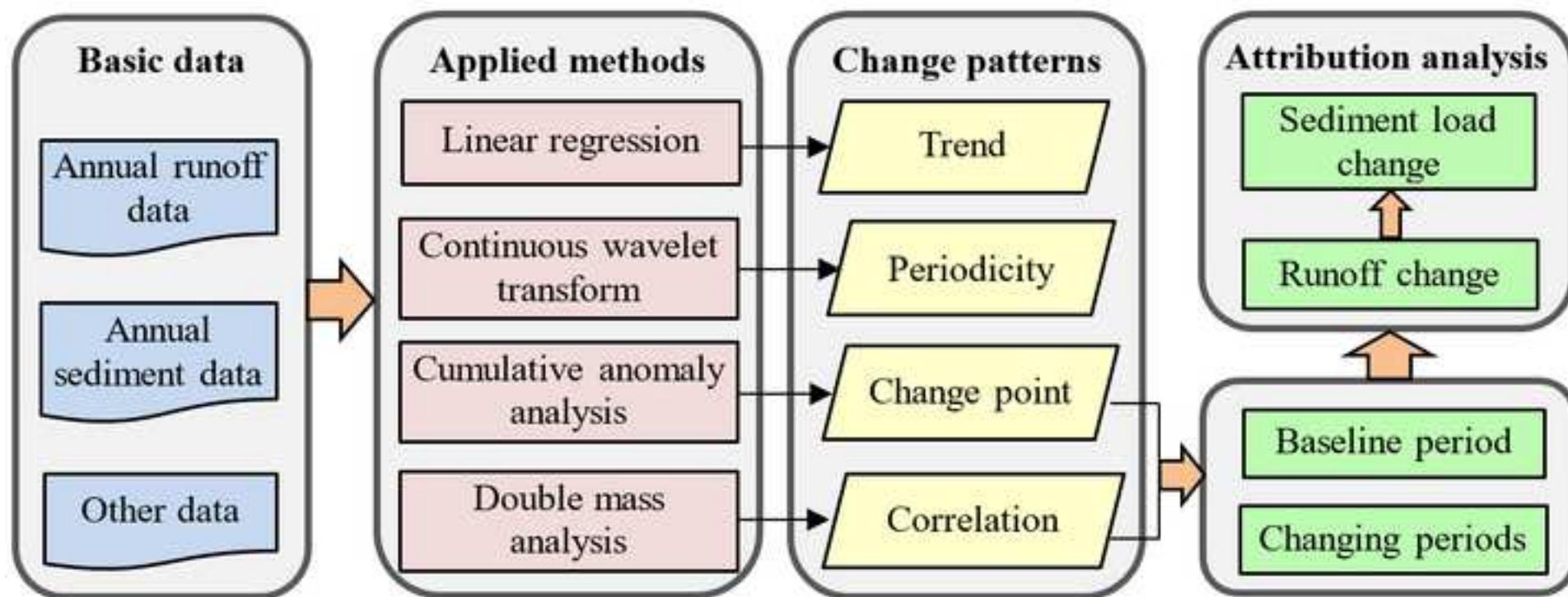


Figure 3
[Click here to download high resolution image](#)

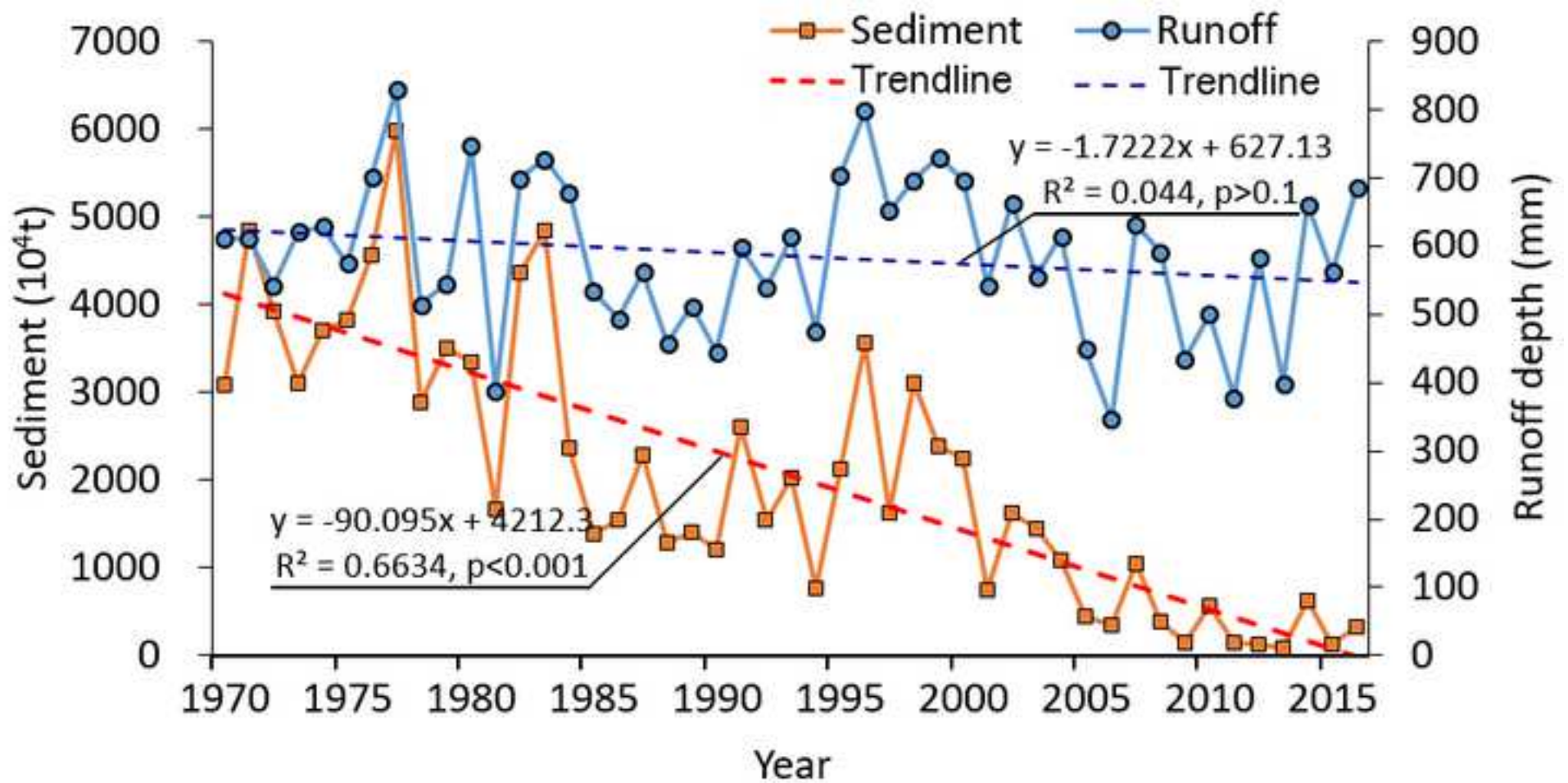


Figure 4
[Click here to download high resolution image](#)

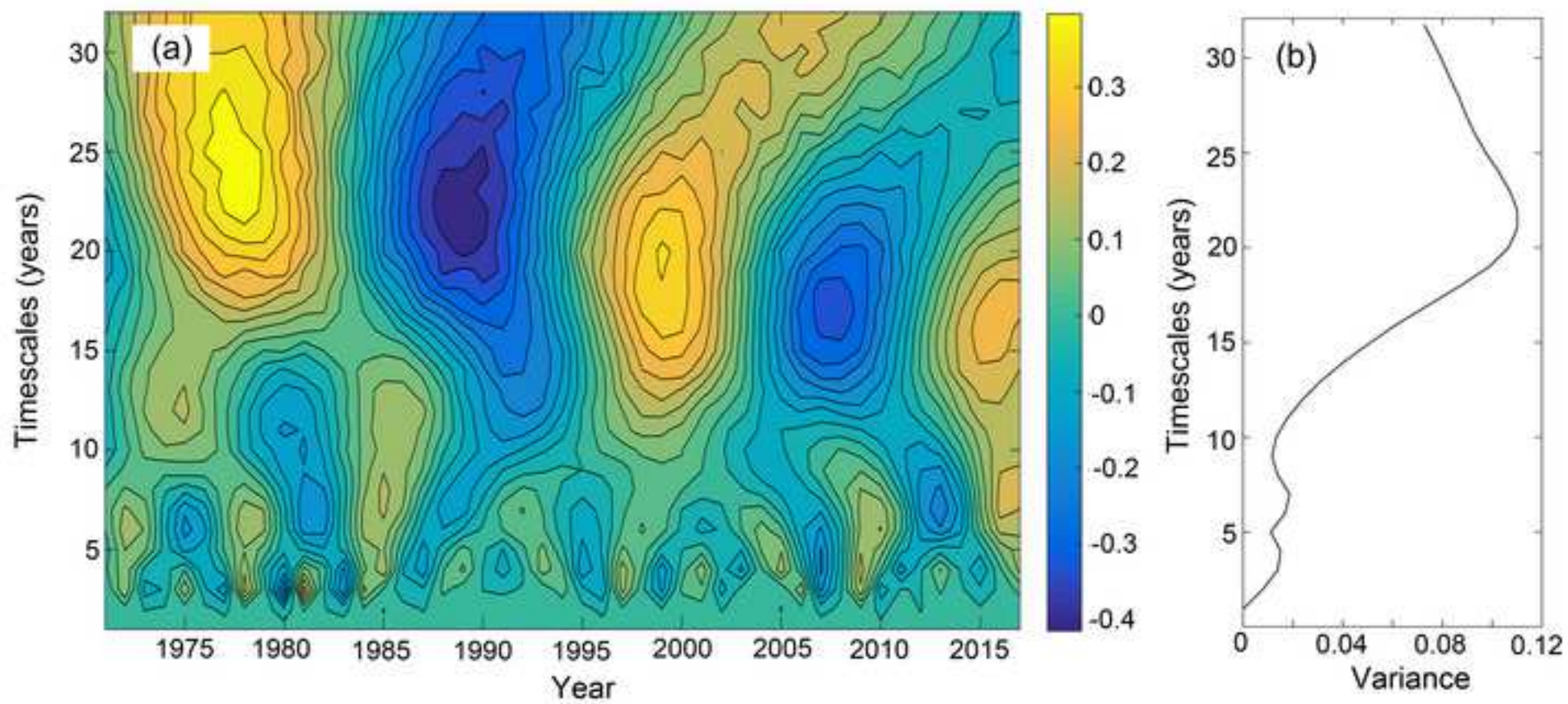


Figure 5
[Click here to download high resolution image](#)

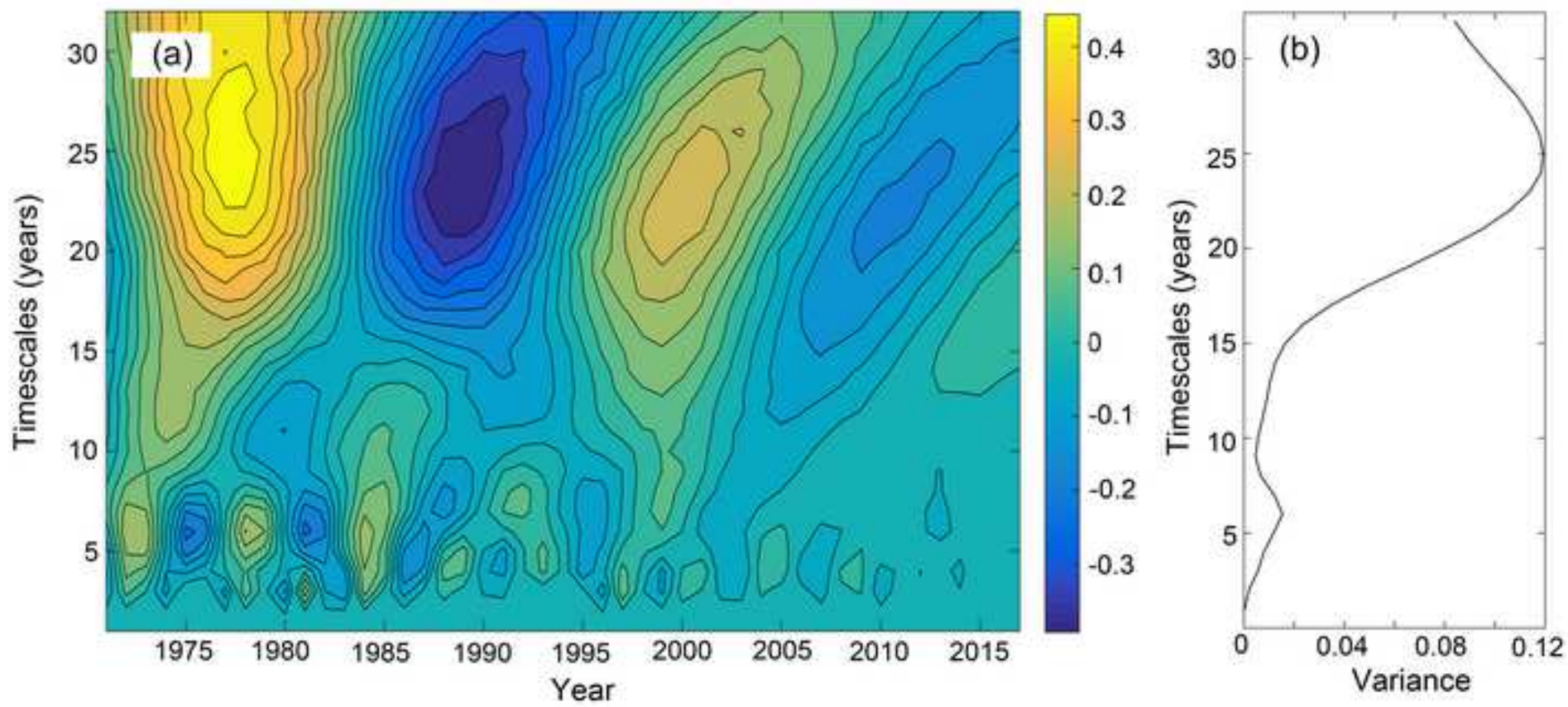


Figure 6
[Click here to download high resolution image](#)

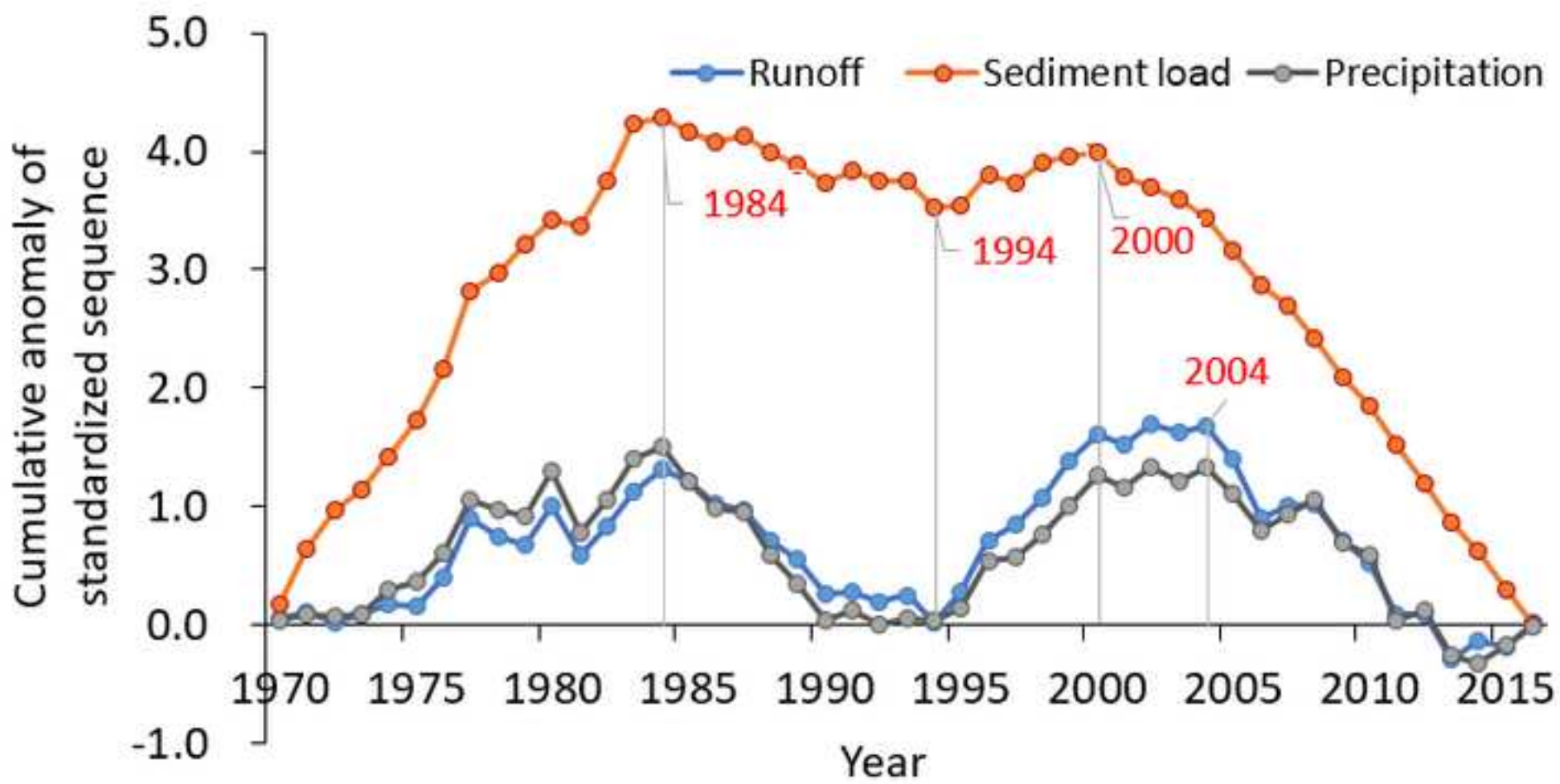


Figure 7
[Click here to download high resolution image](#)

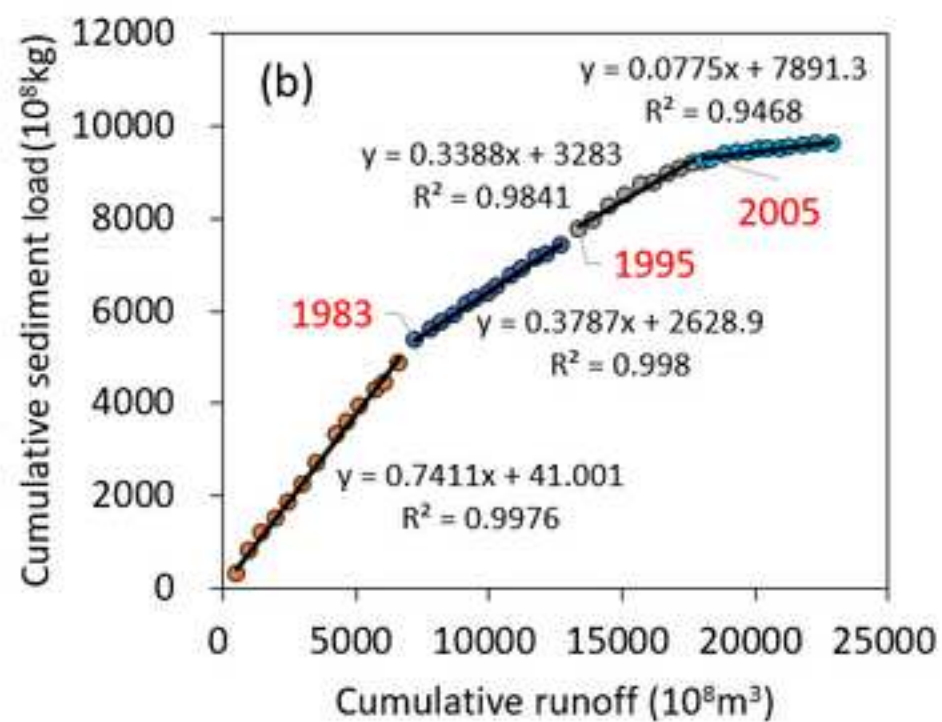
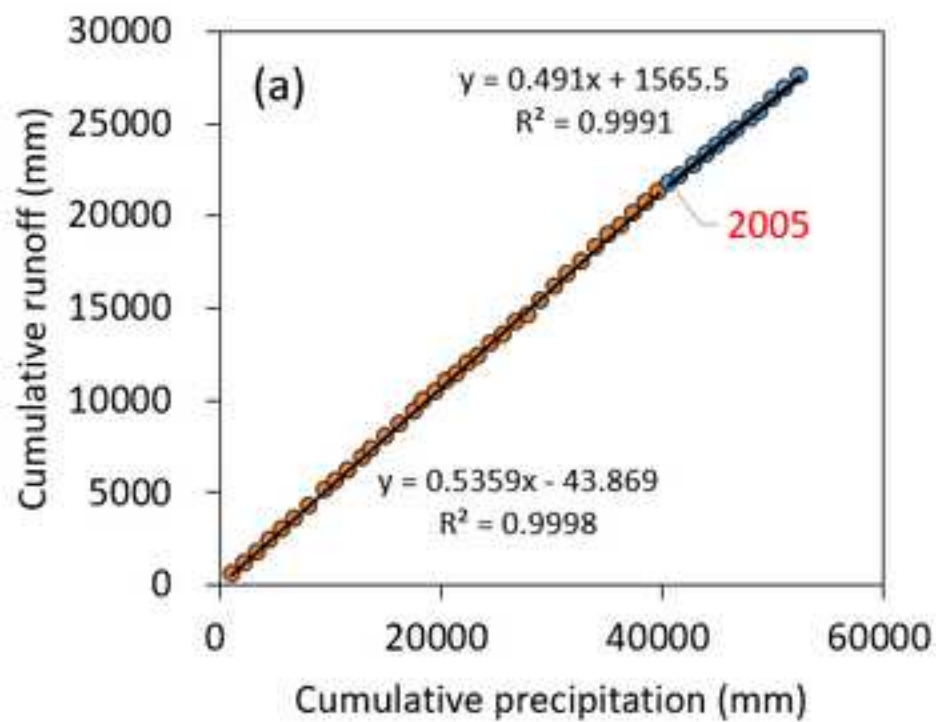


Figure 8
[Click here to download high resolution image](#)

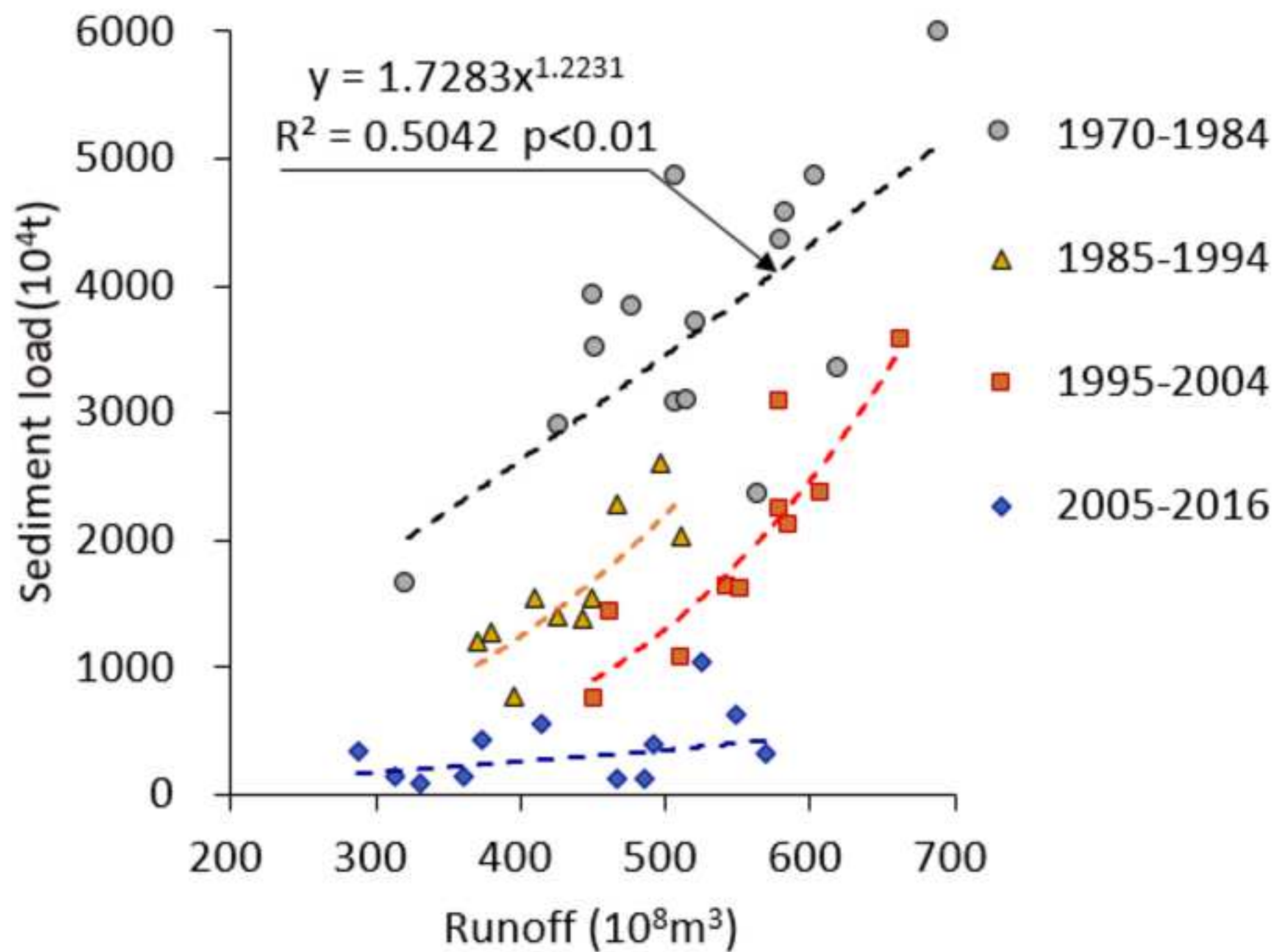


Figure 9
[Click here to download high resolution image](#)

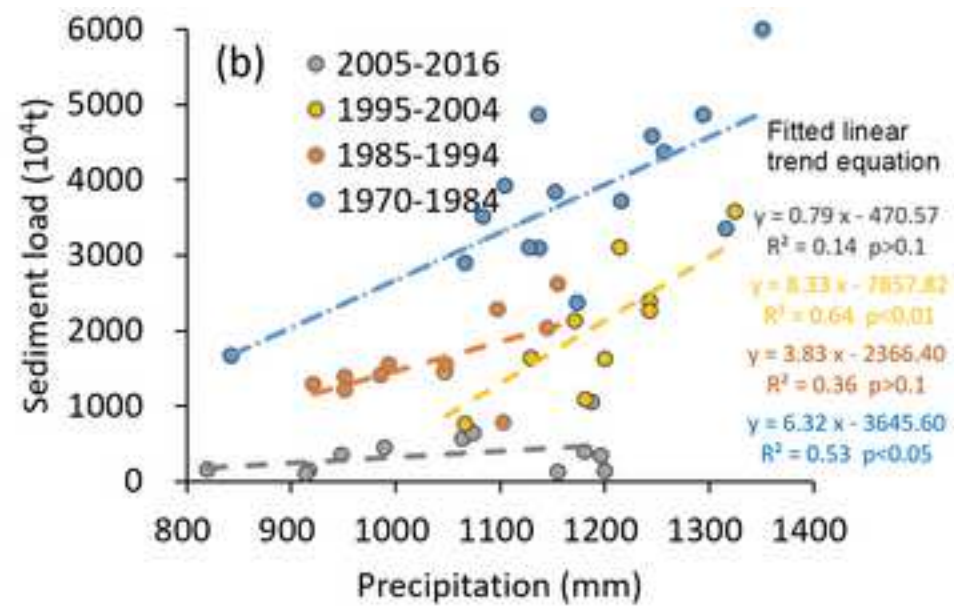
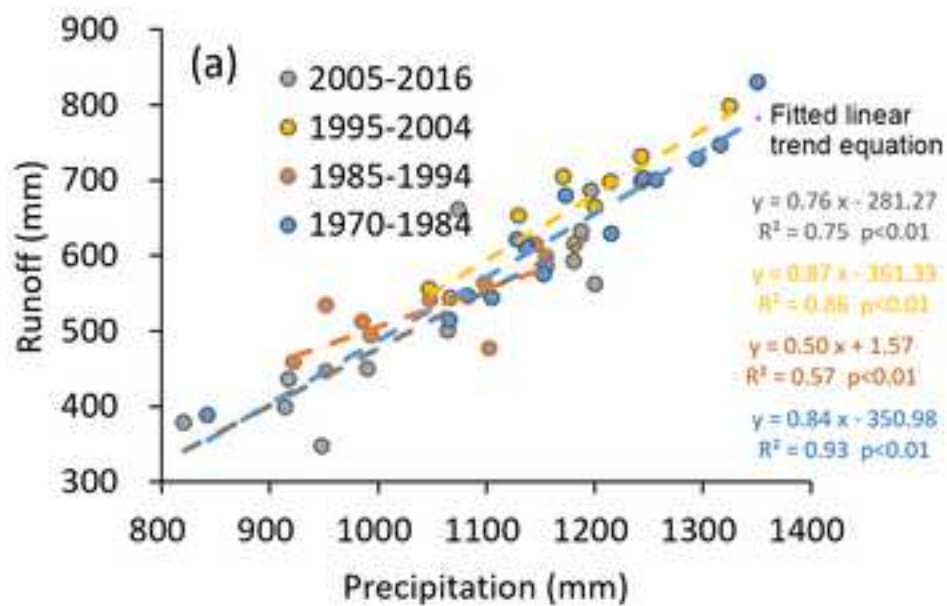


Figure 10
[Click here to download high resolution image](#)

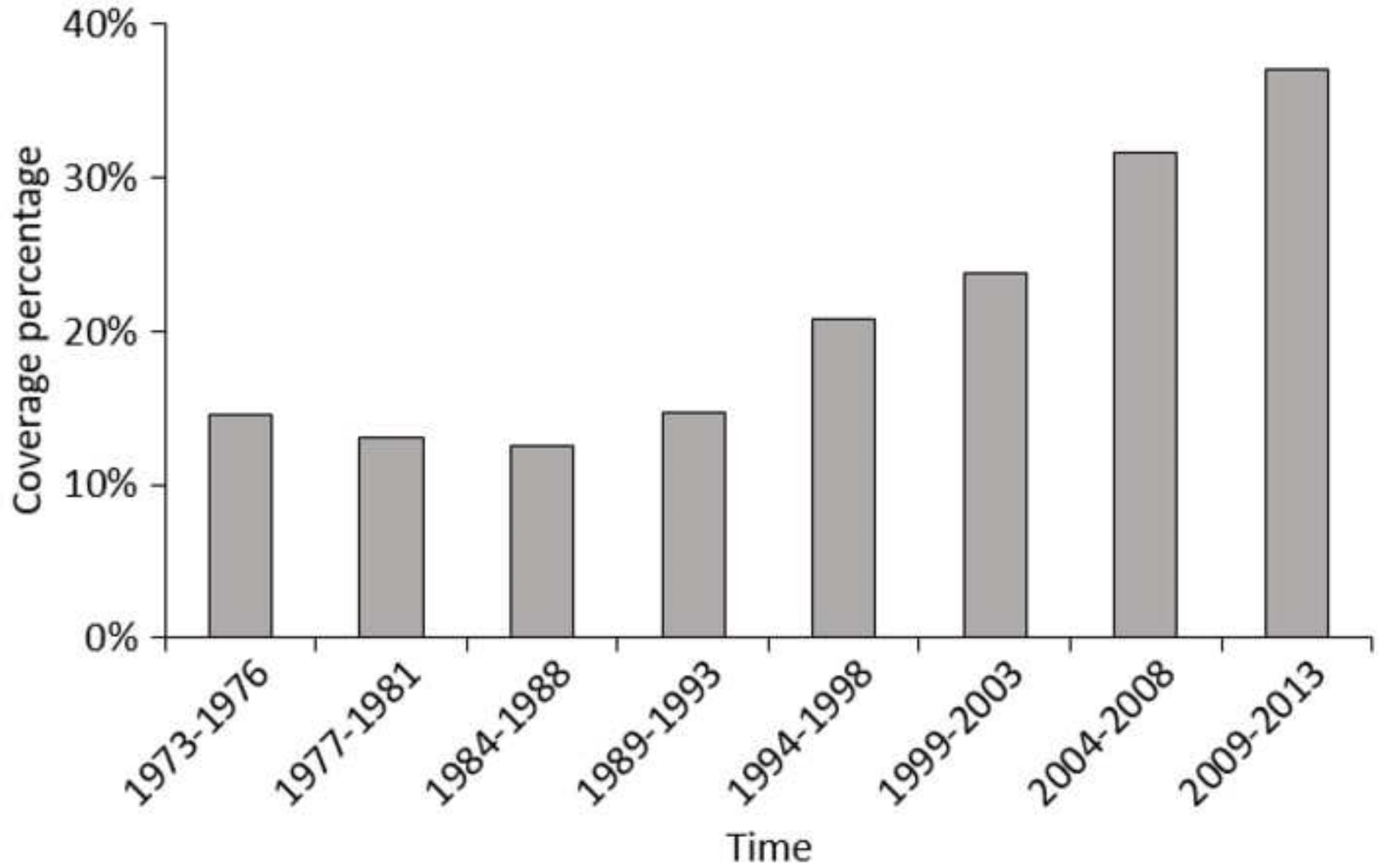


Figure 11
[Click here to download high resolution image](#)

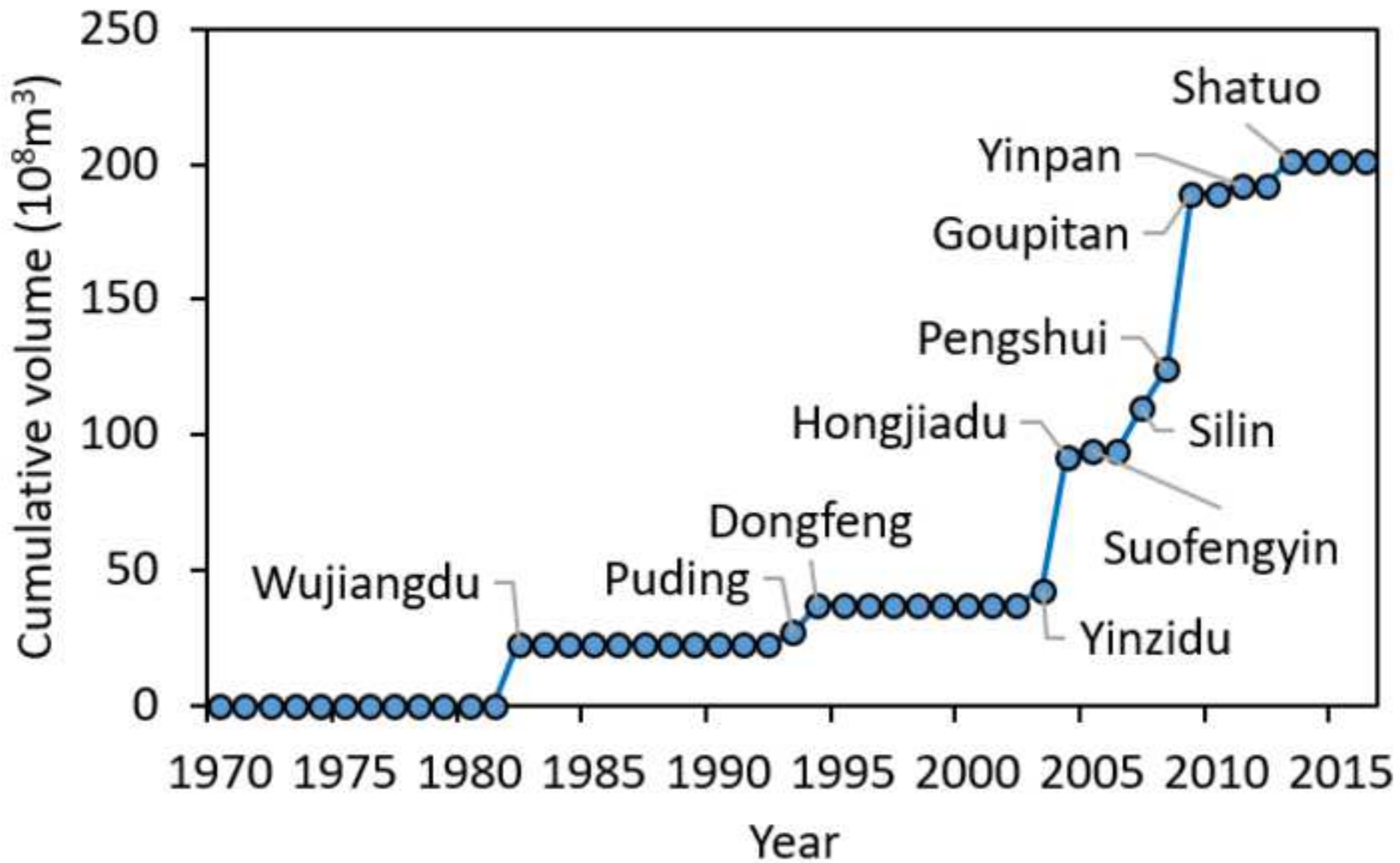


Table 1[Click here to download Table: Table 1.docx](#)**Table 1** Average annual runoff and sediment at Wulong station in four periods

Periods	R (mm)	S (10 ⁴ t)	α (-)	Cs (mg/L)
1970–1984	628.03	3734.00	0.538	716
1985–1994	523.28	1604.00	0.505	369
1995–2004	665.66	1994.00	0.562	361
2005–2016	518.53	363.33	0.491	84

Note: “R” is mean annual runoff depth, “S” is mean average annual sediment load, “ α ” is runoff coefficient and “Cs” is sediment concentration.

Table 2 Impacts of climate variability and human activities on runoff change in the WRB

Periods	R (mm/a)	P (mm/a)	ET _p (mm/a)	ΔR (mm/a)	ΔR _{clim} (mm/a)	ΔR _{hum} (mm/a)	η _{clim-R} (%)	η _{hum-R} (%)
1970–1984	628.03	1167.83	1009.97					
1985–1994	523.28	1035.97	991.51	-104.75	-89.64	-15.12	85.6	14.4
1995–2004	665.66	1183.07	955.00	37.63	26.92	10.71	71.6	28.4
2005–2016	518.53	1054.73	998.97	-109.63	-78.28	-31.22	71.5	28.5

Note: R, P, ET_p are mean annual runoff depth, precipitation and potential evaporation, respectively during the period; ΔR is the change in mean runoff with reference to the baseline period; ΔR_{clim} and ΔR_{hum} are the changes in mean annual runoff due to climate change and human activities as estimated using Equation (3) and Equation (6); η_{clim-R} and η_{hum-R} are the relative contribution rates of climate variability and human activities to runoff change as estimated using Equation (7) and Equation (8).

1 **Table 3** Impacts of climate variability and human activities on sediment change in the
 2 WRB

Periods	S (10 ⁴ t/a)	S _{sim-c} (10 ⁴ t/a)	ΔS (10 ⁴ t/a)	ΔS _R (10 ⁴ t/a)	ΔS _{clim} (10 ⁴ t/a)	ΔS _{hum} (10 ⁴ t/a)	η _{clim-S} (%)	η _{hum-S} (%)
1970-1984	3734.00	3655.04						
1985-1994	1604.00	2916.77	-2130.00	-817.23	-699.31	-1430.69	32.8	67.2
1995-2004	1994.00	3916.06	-1740.00	182.06	130.26	-1870.26	-7.5	107.5
2005-2016	363.33	2898.53	-3370.67	-835.47	-597.28	-2773.39	17.7	82.3

3 Note: S is the observed mean annual sediment; S_{sim-c} is the re-constructed mean annual sediment load as
 4 estimated using Equation (10); ΔS is the change in mean sediment load with reference to the baseline
 5 period; ΔS_R is the change in mean sediment load caused by runoff change as estimated using Equation
 6 (12); ΔS_{clim} and ΔS_{hum} are the changes in mean annual sediment load due to climate change and human
 7 activities as estimated using Equation (13) and Equation (14); η_{clim-R} and η_{hum-R} are the relative
 8 contribution rates of climate variability and human activities to sediment load change as estimated using
 9 Equation (15) and Equation (16).

Figure caption:

Fig. 1. Topography and river networks of the Wujiang River basin, with hydrological stations and meteorological stations are marked. The photos in the right column shows the typical landscapes of the river basin. Hydropower stations in the Figure are: 1 Puding; 2 Yinzidu; 3 Hongjiadu; 4 Dongfeng; 5 Suofengying; 6 Wujiangdu; 7 Goupitan; 8 Silin; 9 Shatuo; 10 Pengshui; 11 Yinpan.

Fig. 2. Flowchart of the method to assess the impacts of climate variability and human activities on runoff and sediment load changes.

Fig. 3. Annual runoff depth and sediment load of Wulong station during 1970–2016.

Fig. 4. Periodicity distribution of Wulong annual runoff based on Morlet wavelet analysis: (a) continuous wavelet power spectrum and (b) wavelet variance.

Fig. 5. Periodicity distribution of Wulong annual sediment load based on Morlet wavelet analysis: (a) continuous wavelet power spectrum and (b) wavelet variance.

Fig. 6. Variation of the cumulative anomaly curves of annual precipitation, runoff and sediment load of the Wujiang basin during 1970-2016.

Fig. 7. The double mass curves of (a) cumulative precipitation versus cumulative runoff and (b) cumulative runoff versus cumulative sediment load of the Wujiang basin.

Fig. 8. Relationship between annual runoff and sediment load in different periods.

Fig. 9. Linear relationship between (a) precipitation and runoff and (b) precipitation and sediment load of the Wulong station.

Fig. 10. Changes of area percentage of forest coverage in the Guizhou Province.

Fig. 11. Variation of cumulative reservoir volume according to the operation of major hydropower stations in the WRB.

Meteorological data

[Click here to download Supplementary material for on-line publication only: Meteorological data.xlsx](#)

Annual runoff and sediment load

[Click here to download Supplementary material for on-line publication only: Annual runoff and sediment load.xlsx](#)

Forest coverage of Guizhou Province

[Click here to download Supplementary material for on-line publication only: Forest coverage of Guizhou Province.xlsx](#)

Hydropower information

[Click here to download Supplementary material for on-line publication only: Hydropower information.xlsx](#)